

# CHALMERS



## **Reliability and economic analysis of offshore wind power systems- A comparison of internal grid topologies**

*Thesis for the Master of Science Degree (MSc)*

**Tomas Winter**

Department of Energy and Environment  
*Division of Electric Power Engineering*  
CHALMERS UNIVERSITY OF TECHNOLOGY  
Examiner: Lina Bertling, Professor  
Supervisor: Francois Besnard, PhD student  
Gothenburg, Sweden, 2011-12-01

## **Abstract**

Wind power has emerged the last decades as an important technology for low carbon emitting electricity production. The development was first onshore, but recently many wind farms have been developed offshore due to space availability, low noise and visual impacts. Offshore wind farms experiences higher winds resulting in higher production, but investment costs, and operation and maintenance costs are also much higher. More specifically, a failure may result in long downtime due to inaccessibility to the site during harsh conditions, and transportation costs are also higher since boats, and sometimes helicopters are necessary.

This study consists of a reliability and economic analysis of the internal grid of offshore wind power system. Different topologies are evaluated and compared against each other with the aim of presenting alternative layouts with increased level of reliability at an acceptable cost. The different layouts are compared in additional income over the life time of the wind farm considering the energy not supplied.

The results show that for the case study consisting of two arrays of ten 3MW wind turbines—three of the proposed alternative layouts presents a positive Net Present Value of the extra investment of 63k€, 165k€ and 201k€ respectively. It can be concluded that it can be beneficial to implement some degree of redundancy along with improvements in the protection system.

# Table of Contents

## ABBREVIATIONS

- CHAPTER 1: INTRODUCTION AND BACKGROUND ..... 1
  - 1.1 Background..... 1
    - 1.1.1 Why constructing offshore wind power plants? ..... 1
    - 1.1.2 Future wind power initiatives ..... 1
    - 1.1.3 Reliability analyses ..... 2
  - 1.2 Scope of the Work ..... 2
  - 1.3 Method..... 3
  - 1.4 Assumptions and scope ..... 4
  - 1.5 Previous work in this area ..... 4
  - 1.6 Outline of the thesis ..... 5
- CHAPTER 2: THEORY ..... 7
  - 2.1 Wind power ..... 7
    - 2.1.1 Basic of wind energy ..... 7
    - 2.1.2 Wind turbines..... 10
  - 2.2 Net present value and the internal rate of return ..... 13
  - 2.3 Power system reliability ..... 14
    - 2.3.1 System analysis ..... 15
    - 2.3.2 Analytical methods and Monte Carlo simulation ..... 16
    - 2.3.3 Reliability indices ..... 16
    - 2.3.4 Series and parallel systems ..... 19
- CHAPTER 3: NEPLAN ..... 22
  - 3.1 NEPLAN Planning and Optimization Software ..... 22
  - 3.2 Fundamental Calculation Flow in NEPLAN ..... 22
    - 3.2.1 Network data input..... 23
    - 3.2.2 Generation of failure combination ..... 23
    - 3.2.3 Overlapping stochastic outages..... 24
    - 3.2.4 Failure effect analysis ..... 26
  - 3.3 Example cases with NEPLAN and analytical calculations without considering load flow ..... 27

3.3.1 Radial network calculations .....	27
3.3.2 Combination of series and parallel network calculations .....	29
CHAPTER 4: OFFSHORE WIND FARM GRID TOPOLOGY.....	32
4.1 Different layouts for offshore collector systems/Common grid topology structures .....	32
4.1.1 Radial design.....	33
4.1.2 Single-sided ring and shared ring design .....	34
4.1.3 Double-sided ring.....	34
4.1.4 Star design.....	35
4.1.5 Single return- or shared ring design.....	36
4.1.6 Double-sided half-ring design.....	36
4.2 Thanet offshore wind farm .....	37
4.2.1 Basic information and location .....	37
4.2.2 Turbines technical specifications .....	38
4.2.3 Internal networks technical specifications .....	39
CHAPTER 5: ANALYSIS OF DIFFERENT TOPOLOGIES .....	41
Alternative layout, Top.1 .....	43
Alternative layout, Top.2.....	44
Alternative layout, Top.3.....	45
Alternative layout, Top.4.....	46
Alternative layout, Top.5.....	46
Alternative layout, Top.6.....	47
Alternative layout, Top.7.....	48
CHAPTER 6: RESULTS .....	48
6.1 Description of the results per topology.....	48
6.2 Results discussion.....	53
CHAPTER 7: CONCLUSIONS.....	55
7.1 Conclusions and discussion .....	55
7.2 Future work.....	55
REFERENCES.....	57

## Abbreviations

EWEA	European Wind Energy Association
HL	Hierarchical Levels
FF	Failure Frequency [1/year]
FD	Failure Duration [hours/year]
SAIFI	System Average Interruption Frequency Index [int./year,customer]
SAIDI	System Average Interruption Duration Index [hour/year,customer]
CAIDI	Customers Average Interruption Duration Index [hour/int.]:
ASAI	Average Service Availability Index [%]
ENS	Energy Not Supplied [MWh/year]
NPV	Net Present Value [k€]
IRR	Internal Rate of Return [%]
AEAE	Additional Expected Annual Energy [MWh/year]
AEI	Additional Expected Income [k€]
WACC	Weighted Average Cost of Capital [%]
DFIG	Double Fed Induction Generator
WRIG	Wound Rotor Induction Generator
O&M	Operations & Maintenance

# CHAPTER 1: INTRODUCTION AND BACKGROUND

## 1.1 Background

The wind power industry is growing rapidly and more wind power plants are being erected offshore with increasing distance to land. Building wind farms offshore is expensive and associated with high maintenance cost. Thus there is a growing interest in performing reliability assessments during the design phase which is the most influential phase for the O&M. This is performed in order to optimize the topology according to its expected economic benefits due to less interruption in energy production. The offshore environment and many of the products are also rather unproved which makes it important to carefully carry out a reliability assessment in order to avoid trial and errors in most possible way. Despite these issues offshore wind power plants also comes with several benefits like higher power production due to stronger winds along with less disturbances to people.

By comparing different topologies of a wind farm it is possible to determine and evaluate the most reliable installation. The reliability study can also highlight weak points within the system which might need improvements in redundancy.

A problem with reliability studies of offshore wind farms is that the existing wind farms do not have so many years of experience. This makes it sometimes difficult to collect trustworthy reliability data suitable for the intended topology.

### 1.1.1 Why constructing offshore wind power plants?

The main reason for building offshore wind farms is the availability of space together with good wind resources. Moreover, it has a lower noise and visual impact which often affect the feasibility of onshore wind farms. For these reasons, offshore wind is important to complement onshore wind, especially in countries where space available for onshore wind farms is limited, e.g. in Germany and Denmark.

### 1.1.2 Future wind power initiatives

All these aspects added together have made the interest of wind energy more topical than ever worldwide. European targets from the European Wind Energy Association (EWEA) have the aim to integrate 230 GW of wind power in the European grid by 2020 of which 40 GW

offshore. In Sweden there is a current planning goal, adopted by parliament in 2002 for wind power of 10 TWh by 2015. Parliament has in June 2009 adopted a new national planning by 2020 to 30 TWh, of which 10 TWh offshore [7].

To reach these goals, it is necessary to have incentives systems for renewable energy since the generation cost from renewable sources is generally higher than conventional energy generation sources such as coal, gas, nuclear and hydro plants. Incentives systems varies much between countries and may be based on fixed feed-in tariffs, or green certificates or a mix [24].

### **1.1.3 Reliability analyses**

Interruption in the power production from an offshore wind farm - will lead to income losses. As a consequence, a goal in designing offshore wind farms is to find balance between the intrinsic reliability together with its costs and the cost of maintenance including the indirect costs of supply interruptions.

A reliability study provides results which can give an appropriate benchmark for assessing the system performance and identifying the weak points of the system. With increased knowledge of weak points within the system, informed investment decisions can be made during the design phase. This action can reduce further costs due to supply interruptions and also decrease the need for maintenance. Thus there is of great importance to identify the weak spots and reinforcing them in order to achieve higher reliability and decrease the probability of interruptions. A wind farm has an inborn stochastic characteristic and it is difficult to guarantee continuous supply but the probability or duration of interruptions can be reduced during its planning stage. This is though always a balance between the reliability assessment and investment cost. Are the investments in improvements considered to pay off in the long run?

## **1.2 Scope of the Work**

The objective of this thesis is to perform a quantitative reliability analysis of the internal grid of an offshore wind power system, comparing different topology and their economic benefits.

The case study is based on an existing 300 MW offshore wind farm named Thanet which is located in the North Sea just off the Kent coast in UK. The structure of this wind farm was studied and simplified to create a base case for the purpose of this work. Real data from this

existing wind farm has been used which provides a good added value to the study. Different topologies is evaluated and compared against each other. The aim is to present alternative layouts with increased level of reliability at an acceptable cost. The different layouts can be compared in additional income over the life time of the wind farm, as the energy not supplied (ENS) is used in the study.

### 1.3 Method

In order to evaluate different topology alternatives of the modeled part of the wind farm, the software NEPLAN is used to perform reliability analysis while considering power flow in order to check that the cable constraints are not violated. To perform a reliability assessment, NEPLAN simulate the reliability for each component in the system, with failures up to second order (i.e. two failures simultaneously), determines the impact of each contingency to each load point, determines the frequency of production interruption and sums up the impact of all contingencies for an overall reliability assessment.

The approach chosen to model the wind farm in NEPLAN, is to represent the feeding grid as one ideal generator and model all the wind turbines as loads. This was necessary to be able to model partial reduced production of the wind turbines when the capacity of some cable cannot take the whole production. The outage duration at each turbine can then be calculated by NEPLAN and the outage duration of the whole wind farm is taken as an average of the values obtained for each of the wind turbines.

In order to analyze improvements in reliability on the different layouts, the original topology is modified. This is performed by adding remote controlled load switches, including cable loops and/or changing cable dimensions within the system. Each and every topology is analyzed, documented and compared with the original layout as a benchmark.

The data used in the report is collected from various sources like Vattenfall, Prysmian, Siemens and ABB. There have been some difficulties to collect all the relevant data for the study, especially regarding costs and failure rates, and different complementary sources have been used [6], [10], [26].

NEPLAN can perform an investment analysis and calculate the net present value (NPV) of different investment alternatives. In order to have full overview over the calculations and the varying input parameters for different topologies, it was chosen instead to perform these calculations using Microsoft Excel. Besides NPV, the internal rate of return (IRR) is also

calculated for each topology alternative. Both NPV and IRR are very easy to calculate with predefined equations in Excel and the results can be visualized in tables and graphs.

#### **1.4 Assumptions and scope**

The study is performed on two rows including each ten turbines with equally distance between turbines and rows. This model is supposed to symbolize two branches on the existing wind farm Thanet. Data on components included in the model, such as turbines, switching devices and cable dimensions, are real data collected from Thanet. In the real wind farm the rows and turbines are not total evenly distributed with ten turbines in each row and exact distances between- each other and to the offshore platform. This is although a good approximation for the study. There is an offshore platform with two transformers situated in the middle of the wind farm and the connection bus on the platform is the physical outer limit of the study.

The purpose of the study is to evaluate the reliability improvements on different topology alternatives. This is performed by adding remote controlled load switches, including cable loops and/or changing cable dimensions within the system. This makes the relevant reliability data needed for the system limited to include switching devices and cables. Because of that the turbines and the platform bus are modeled as ideal elements. Another aspect to consider is that it is difficult to find reliable and relevant data.

When assessing topologies with different cable ratings, the vessel cost for burying the cables under the seabed, is not considered since it is already paid once. This cost is although considered when implementing new cables like a loop between the arrays.

The software NEPLAN is used in order to assess the reliability of different topologies with consideration for power flow constraints on the cables, which was performed by power flow analysis. For the study the generators in the wind turbines are modeled and represented as loads using a reverse power flow approach. The software has some limitations which are considered in the study. NEPLAN cannot handle dynamic loads with varying output power and therefore, many cases with constant power have been used in the reliability calculations.

#### **1.5 Previous work in this area**

There have been a number of studies conducted within the area of reliability analysis on power systems and offshore wind farms. There is for example one study which is focusing on

reliability assessments in the power system [9]. The basic theory of the report is providing the same basic understanding of how reliability calculations are performed during a reliability study in power systems. The report also uses the software NEPLAN as a tool for calculations.

Other example of studies evaluating the reliability of offshore wind farms is [6] which performs a reliability study with an analyses of electrical system within offshore wind parks, [10] which performs a reliability and investment analysis of different layouts on the Lillgrund wind farm and [11] which performs a reliability analyses of collection grids for large Offshore wind farms.

A common factor for all these reports is that reliability analysis is performed without considering possible overflow in cables due to re-routing of the power. When evaluating topologies with increased reliability due to implementing redundancy, it is important to consider the increase in power transferred within the remaining cables in case of failure. Without considering this factor, a proper reliability benefit of redundancy with respect to cable size cannot be performed.

Another aspect to consider is that the wind turbines are not producing energy continuously at their average capacity factor (i.e. 40% of rated capacity) but their production varies continuously. This implies that it may not be necessary to dimension the cables used for redundancy to handle full production, since the full production condition occurs only for a low percentage of the time. The design should be a balance between several factors such as: probability of wind speed, probability of failure, cost of material, increase in energy supplied and life time of wind farm.

As a result of the identified weaknesses in previous studies, it was decided to perform a reliability analysis considering both possible cable overload and impact of wind regimes.

## 1.6 Outline of the thesis

**Chapter 2** explains the underlying theory used for the study. The chapter describes some fundamentals of wind power followed by theory used for investment analysis. The chapter concludes with an overview of the basic concepts in evaluating power system reliability.

**Chapter 3** provides a practical understanding of how reliability calculations are performed during a reliability study in power systems using the software NEPLAN.

**Chapter 4** illustrates the current state of art in grid configuration of offshore wind farms along with alternative layouts for offshore collector systems. This is followed by a brief description of the Thanet wind farm and its included components.

**Chapter 5** presents the data used for the models and the different topologies chosen for the analysis. Some drawbacks and benefits are also discussed for each topology.

**Chapter 6** presents and visualizes the results obtained from the simulations on different topology alternatives in NEPLAN.

**Finally, Chapter 7** concludes the thesis, summarizes the results, presents some ideas and discusses future work.

## CHAPTER 2: THEORY

---

*The beginning of this chapter describes some fundamental knowledge on wind power which is followed by theory used for investment analysis. The last section in this chapter provides an overview of the basic concepts in evaluating power system reliability.*

---

### 2.1 Wind power

#### 2.1.1 Basic of wind energy

##### Power in the wind

According to the first law of thermodynamics energy can neither be created nor destroyed, it can only be transformed from one form to another. The power content in the wind can be calculated as:

$$P_{wind} = \frac{1}{2} \rho v^3 \quad (1)$$

Where:

$P_{wind}$  : Power [W]

$\rho$  : Density of air [kg/m<sup>3</sup>]

$v$  : Wind speed [m/s]

The energy flowing through the rotor is then the product of the wind power and the area of the rotor. Due to constraints on the continuity of flow, the maximum power that can be extracted from the wind is limited by Betz law. However in the practice it is lower due to aerodynamic and drive train losses. Moreover, the energy extracted will depend on tip speed ratio (ratio speed, rotor hedge and wind speed) which often vary with the wind speed, and it is limited by the installed capacity of the wind turbines.

$$P_{turbine} = \frac{1}{2} \rho v^3 C_P A_R \quad (2)$$

Where:

$C_P$  : Coefficient of Performance. The coefficient of performance is limited by Betz law ( $16/27 \approx 59.3\%$ ); However it is lower due to stated limits and will vary depending on the tips

speed ratio (ratio speed rotor hedge and wind speed) so it is not a unique number for one wind turbine but rather depends on the wind speed and type of power control.

$A_R$ : Rotor swept area [ $m^2$ ]

### Power curve

The power curve models the power output for a specific wind turbine as a function of wind speed. This curve is not linear with wind speed and the shape varies between different types of wind turbines. The power curve derives directly from  $C_P$  which is the wind turbines efficiency coefficient.  $C_P$  increases with the wind speed up to its maximum and decreases with higher wind speed in order to limit the output power to the rated level. The power curve is illustrated in Figure 1:

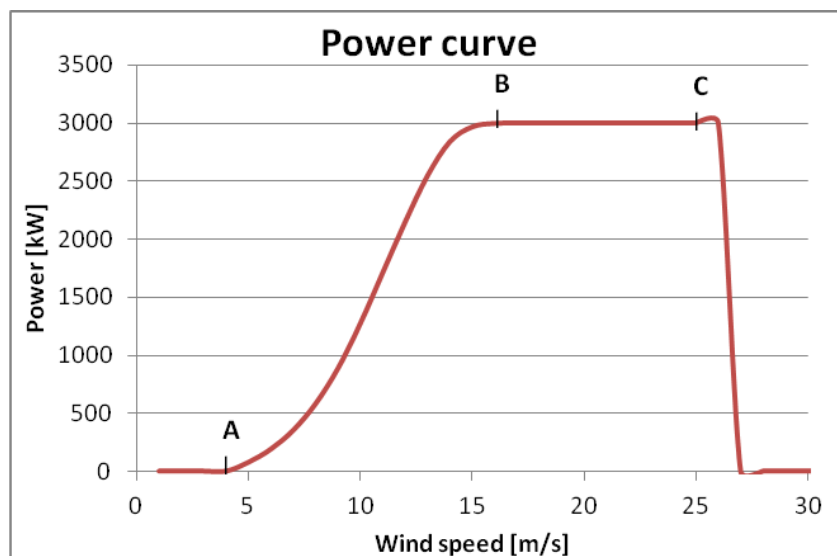


Figure 1. The power curve of the Vestas V90 3MW turbine [13]

- Point A is cut-in wind speed.
- At Point B the wind turbine reached rated power.
- Point C is cut-out wind speed.

The turbine has a cut-in wind speed (point A in Figure 1) where it starts to generate electricity. After the cut-in wind speed the generation of power increases significantly with higher wind speeds up to point B (Figure 1), where it reaches the rated power of the turbine. After point B the power production is constant for higher wind speeds until it reaches the cut-out wind speed at point C (Figure 1). The turbine rotation is stopped at “cut-out” wind speed

because of safety reasons. In order to calculate the average power production of the wind turbine, the product of the probability density function of the wind speed and the turbine's power curve are integrated [14], [15].

### Wind Resources

By looking at equation 1 and 2 it can be determined that a small change in wind speed contribute to a large change in power. A double in wind speed provides eight times the power content. Because of this it is very important to evaluate the wind conditions at the site, when planning a wind farm. At most sites worldwide the wind follows the Weibull- or the simplified Rayleigh distribution. When using the Rayleigh distribution for modeling the probability of the wind at a specific site, the only parameter which has to be known is the average wind speed. The probability distribution,  $P(v)$ , of the wind speed,  $v$ , has the following form:

$$P(v) = \frac{v}{\sigma^2} e^{-\frac{v^2}{2\sigma^2}} \quad (3)$$

$$\sigma = \frac{v_{Avg}}{\sqrt{\frac{\pi}{2}}}$$

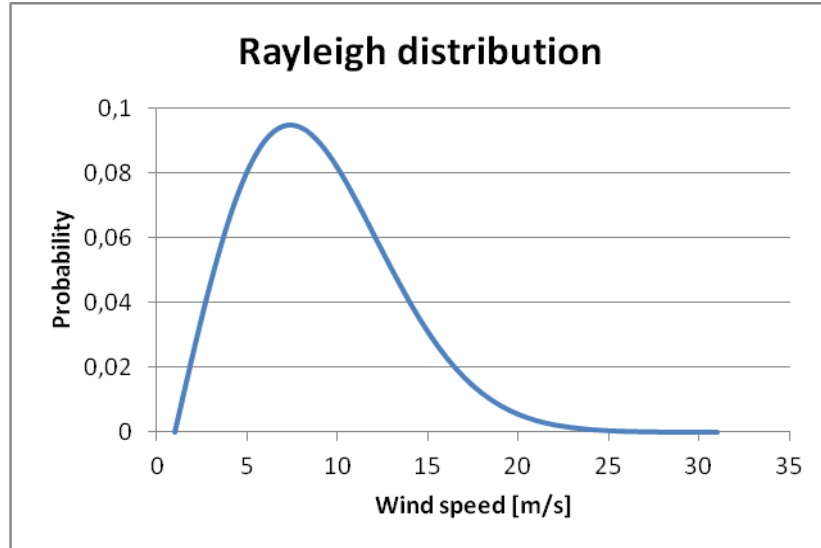
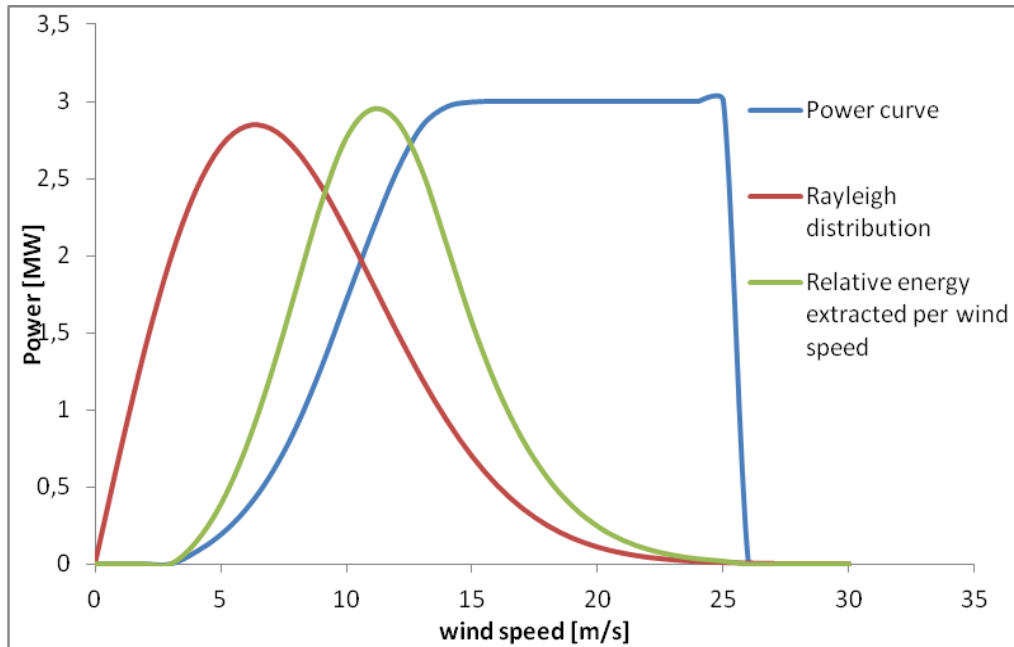


Figure 2. Probability density function of a Rayleigh distribution with the mean speed 8 m/s

### Production estimates

The wind forecasts and production estimates of a wind farm are very dependent of the weather and it fluctuates over the seasons. Figure 3 below shows how the wind resources, power curve and capacity factor are linked together by implementing them in the same graph. As mentioned before, the average power production of the wind turbine is calculated by

integrating the product of the probability density function of the wind speed and the turbine's power curve. This is pictured in the graph as the relative energy extracted per wind speed.



**Figure 3.** The picture shows: the power curve of the Vestas V90 3MW turbine, the probability density function of a Rayleigh distribution with the mean speed 8 m/s and the relative energy extracted per wind speed.

The ability for a wind turbine to deliver energy over a selected period is called the capacity factor  $C_f$ . The capacity factor is defined as the ratio between the average power production of the wind turbine and the rated power of the wind turbine. The equation below shows how the capacity factor is calculated by dividing the expected energy production in a year with the rated energy of the turbine.

$$C_f = \frac{E_{expect}}{E_{rated}} = \frac{P_{turbine} * 8760}{P_{rated} * 8760} = \frac{\frac{1}{2} \rho v^3 C_P A_R}{3MW}$$

### 2.1.2 Wind turbines

A wind turbine converts kinetic energy of the wind into mechanical energy and further into electrical energy. The wind turbine captures the wind energy with the blades and converts the wind power into mechanical rotational energy. The wind turbine can be equipped with different number of blades and the amount depends on the location and application. Figure 4 shows a common setup of components included in a wind turbine.

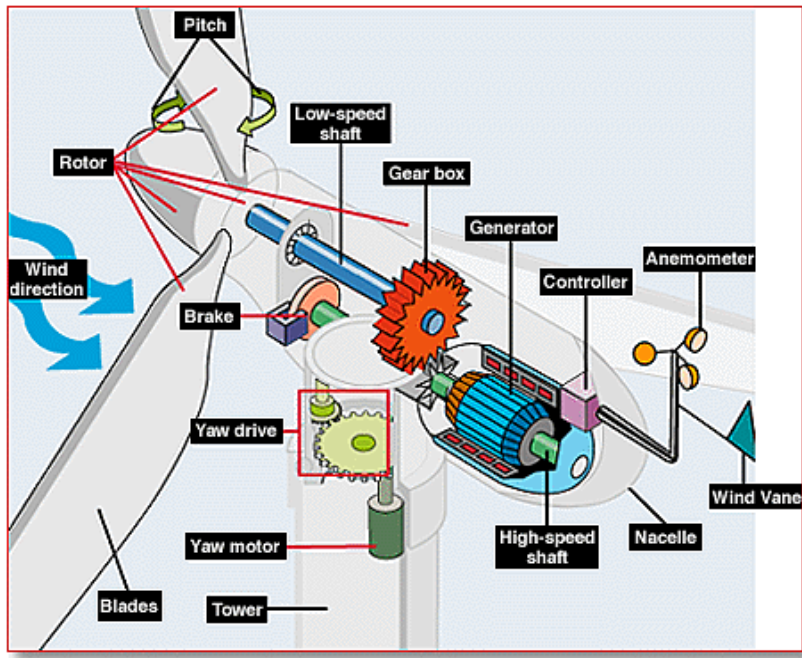


Figure 4. Common setup of components included in a wind turbine. [19]

## Blades

The rotational speed is limited by the number of blades and fast running rotors should have few blades [16]. When generating electricity the generator need high speed at low torque. For this reason most wind turbines used for this application are equipped with two or three blades. Turbines with two blades has lower investment cost and the rotor speed is slightly higher than the equivalent three bladed turbine. Two blades wind turbines are also subject to higher mechanical forces variations on the drive train during one rotation. The motion of a three bladed turbine is steadier and they are visually more accepted, the slightly lower speed also contributes to less aerodynamic noise. As a consequence of, the three-bladed turbine has become the norm, at least for onshore applications. For installations offshore the two bladed versions might be considered in the future due to less investment cost, lighter weight and less visual- and noisily impact on the public. The blades can be made of different materials and the combination varies with turbine size. For larger wind turbines, like the 3 MW Vestas V90 turbine, fiber glass reinforced epoxy and carbon fibers, is used [13].

## Power control

Stalling or pitching are two different ways of controlling the angle at which the wind strikes the blades. This is called controlling the angle of attack and is used for limiting the power in cases where the wind speed exceeds the rated limit of the turbine.

Stalling is a passive approach of controlling the angle of attack by aerodynamically designing the blades. When the wind speed exceeds the rated limit, the angle of attack is increased and some of the wind flow is replaced by turbulence which decreases the lifting force.

Pitch control is an active approach where an electronic controller senses the power output from the turbine and directly pitches the blades out of the wind in case of unsafe wind speeds. This approach provides a better control of the output power and all large modern turbines are using pitch control [14], [15].

### **Gearbox**

In order to increase the speed of the shaft and make the rotational speed suitable for the generator, many turbines use a gearbox. A gearbox consists of many moving parts which are a risk of failure. To reduce friction and mechanical losses, the moving parts in the gearbox are embedded in oil. In the case where the turbines use a direct drive generator, capable of producing electricity at low rotational speed, the gearbox can be excluded [14], [15].

### **Generators**

A typical large wind turbine has either an induction- or synchronous generator for converting the kinetic energy into electrical energy. Synchronous generators are until now quite rarely used because of large size and the need for expensive minerals for the permanent magnets. The benefit of a synchronous generator is that it can extract power from low rotational speeds with high torque which makes it suitable for gearless wind turbines [14].

### **Power converter**

Many wind turbines operate at variable speed in order to improve the performance of the wind turbines. This is performed by keeping the tip speed ratio at a given wind speed as close to the design tip speed ratio at which the efficiency of the turbine is optimized. As a result the generator produces electricity with variable frequency. It is therefore necessary that power electronics are used to match voltage- and frequency level to the one of the grid. The power converter controls the current by using AC/DC and DC/AC converters which also make it possible to control active- and reactive power up to certain limits. The rating of the power electronics depends on the type of wind turbines; e.g. DFIG have only 30% rated power electronics [15], [16].

### **Transformer**

In order to reduce power losses and cable dimensions during transmission, a transformer is used in the wind turbine to increase the voltage level of the electrical power. The transformer can either be located in the nacelle or in the bottom of the tower. In larger offshore wind farms there is mostly an offshore platform with additional high voltage transformers to further increase the voltage before distributing the power to shore [15].

### **Circuit breaker**

In order to protect the wind turbine and its components during faults and short circuits, a remotely controlled circuit breaker is installed between the generator and transformer, and between the transformer and internal grid. Once the fault has been cleared the circuit breaker can be reset and the turbine can operate again [15].

### **SCADA**

A wind turbine is monitored by a SCADA system (Supervisory Control and Data Acquisition) which makes it possible to monitor and control the system. The circuit breakers are operating independently from the SCADA, but the SCADA system can control the opening of the circuit breaker [15].

## **2.2 Net present value and the internal rate of return**

Net present value (NPV) is a method which discounts future cash flows into a present value. NPV compares the value of a Euro today to the value of that same Euro in the future, taking inflation and returns into account. NPV is used in capital budgeting to analyze the profitability of an investment or project. If the NPV of a prospective project is positive, it should be accepted. However, if NPV is negative, the project should probably be rejected because cash flows will also be negative. NPV analysis is sensitive to the reliability of future cash inflows that an investment or project will yield. The NPV shows the present value of future cash flows of an investment, minus the initial investment. This can be an indicator of how much an investment adds to the value of a company. Any project with positive NPV should be considered for investment [29].

$$NPV = \sum_{t=1}^T \frac{C_t}{(1+r)^t} - C_0 \quad (4)$$

Where:

r: Discount rate (the rate of return that could be earned on an investment in the financial

markets with similar risk also known as Weighted Average Cost of Capital - WACC)

T: Time of the cash flow

$C_t$ : Net cash flow (the amount of cash, inflow minus outflow) at the end of year t

$C_0$ : Initial investment cash outlay

The internal rate of return (IRR) is the discount rate that results in a net present value of zero for a series of future cash flows. IRR is just like NPV an approach to evaluate whether an investment is beneficial or not. The difference between the IRR and NPV is that IRR is the true interest yield expected from an investment expressed as a percentage while the NPV is expressed in monetary units like for example Euro's. When comparing different investment alternatives the project with the highest IRR should be chosen [29].

### 2.3 Power system reliability

Reliability is a term which is generally referred to the ability of a system or component to perform in intended manner [1]. In a power system, reliability refers to the ability of the system to satisfy the load demand. The reliability assessment of a power system can be divided into two main aspects which are system adequacy and system security.

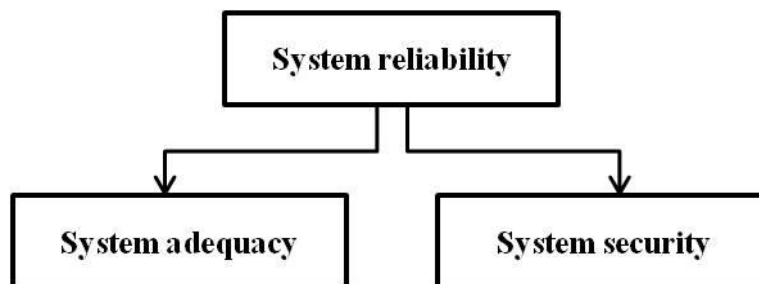


Figure 5. Subdivision of system reliability [2]

The system adequacy evaluates whether there are sufficient facilities within the system in order to fulfill the system operational constraints and load demand of the consumer. The considered facilities related to system adequacy are everything from generating required amount of energy in order to satisfy the consumer, to transmission and distribution facilities

needed for transporting the energy to the load point. One can say that adequacy is associated with static conditions [1], [2].

System security considers the system ability of responding to dynamic or transient disturbances arising within the system. These disturbances include local and widespread failures along with abrupt losses of generation or transmission facilities. Combined or alone these disturbances can lead to dynamic, transient or voltage instability of the system.

For the overall system function these two concepts are dependent of each other but in terms of reliability evaluation they are treated separately and the evaluation is conducted in only one of the domains. In most cases, along with this report, the focus lays on system adequacy for conducting reliability analysis in power systems.

### 2.3.1 System analysis

Because power systems are very large and complex it is very difficult to perform an adequacy analysis on the whole system. Therefore the system is divided into smaller segments while performing adequacy assessment. These segments can be defined as functional zones of generation, transmission and distribution [1], [2]. Evaluation of system adequacy can be performed in each of these functional zones or at hierarchical levels (HL) obtained by combining them with each other. The focus in this study is however on generation and grid connection to the transmission system, which corresponds to the HL1.

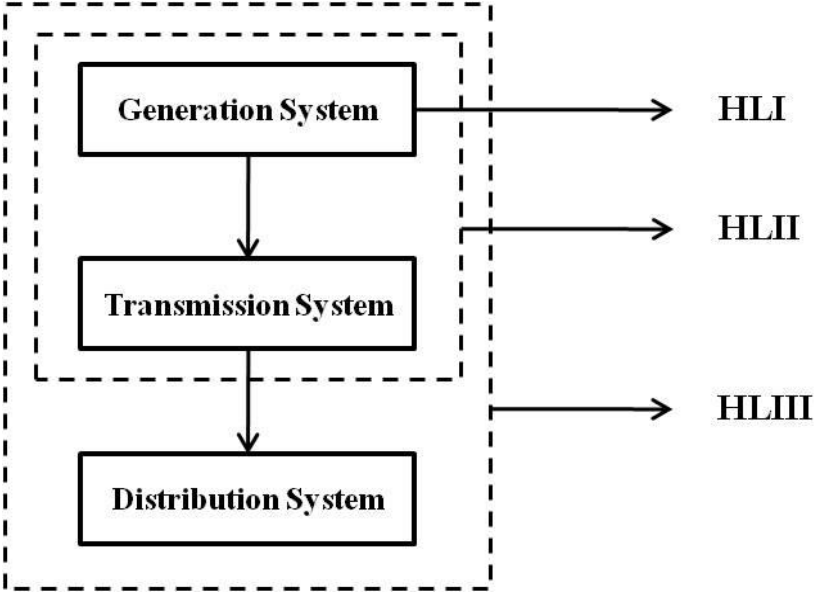


Figure 6. Hierarchical levels [1], [2]

### 2.3.2 Analytical methods and Monte Carlo simulation

Power system reliability evaluation can be performed using analytical methods or Monte Carlo simulation, where the results, in both cases, are numerical parameters in form of reliability indices. These indices represent the capability of the system to provide the customers by acceptable level of supply. Analytical techniques represent the system by mathematical models and evaluate the reliability indices from these models using numerical solutions. The Monte Carlo simulation estimates the reliability indices by simulating the actual process and random behavior of the system. This method is more flexible and precise than the analytical technique but it is more computational intensive [5]. In this work, NEPLAN software was used which implements an analytical method.

### 2.3.3 Reliability indices

In order to perform a reliability assessment a first step is to transform the physical system to an appropriate and simple model. This system model can e.g. be generated by using the stochastic and memory less Markov process. In this process the present state of the system depends on the immediately preceding event but is independent of all former states.

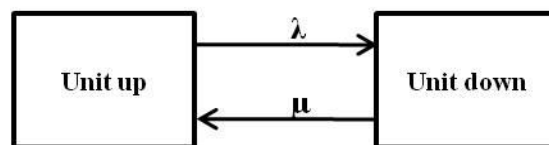


Figure 7. Markov two state model for one unit [1]

The basic two-state reliability model for a power system component is shown in Figure 7 and the state of the unit can be either in- or out of service. The state of the system can be pictured as a binary process. The probabilistic failure frequency for a certain unit is called failure rate and is denoted  $\lambda$  [1/year] and the outage time for a unit in its failure state is denoted  $\mu$  [hour/failure] [1].

By multiplying the failure rate  $\lambda$  with the outage time  $\mu$  and dividing them with the number of hours per year, we get the total unavailability per year in percent for one component.

$$U = \frac{\lambda * \mu}{8760} * 100 \quad (5)$$

For independent outages this model can be expanded to apply for system including two repairable independent components (which corresponds to a second order failure). Component out of service can be a result of forced outage or planned outage due to maintenance. The state space diagram for a set of two components considering independent failures is shown in Figure 8.

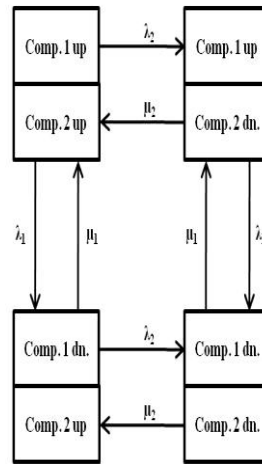


**Figure 8. State space diagram of two repairable components [4]**

where,  $\lambda_i$  and  $\mu_i$  are the failure rate and repair rate of component  $i$  respectively.

These models can be considered when performing a reliability assessment on a wind power plant. The components in the models can e.g. be cables or protections system of the internal grid.

By calculating the failure rate, outage time and unavailability per year one does not take into account the number of affected customer or the quantity of the load loss at failed units. Thus there are different reliability indices that reflect the capability of the system to provide its customer with an acceptable level of supply. There are different indices related to different hierarchical levels of the power system. When analyzing the reliability of the whole power system, there are some customer related indices which are presented in the following [1].

System Average Interruption Frequency Index (SAIFI) [int./year,customer]:

$$SAIFI = \frac{\text{Total Number of Customer Interruption}}{\text{Total number of Customer Served}} = \frac{\sum \lambda_i N_i}{\sum N_i} \quad (6)$$

System Average Interruption Duration Index (SAIDI) [hour/year,customer]:

$$SAIDI = \frac{\text{Sum of Customer Duration Interruption}}{\text{Total number of Customer Served}} = \frac{\sum U_i N_i}{\sum N_i} \quad (7)$$

Customer Average Interruption Index (CAIDI) [hour/int.]:

$$CAIDI = \frac{\text{Sum of Customer Duration Interruption}}{\text{Total number of Customer Interruption}} = \frac{\sum U_i N_i}{\sum \lambda_i N_i} \quad (8)$$

Average Service Availability Index (ASAI) [%]:

$$ASAI = \frac{\text{Customer hours of Available Service}}{\text{Customer hours Service Demands}} = \frac{\sum N_i \cdot 8760 - U_i N_i}{\sum N_i \cdot 8760} \quad (9)$$

Where,  $N_i$  represents the number of customer at load point  $i$ ,  $\lambda_i$  [1/year] is an expected failure rate per year at load point  $i$ ,  $U_i$  is the unavailability of load point  $i$ .

These indices are mainly intended for power system analysis but the ASAI may also be useful when analyzing a wind farm. Either the whole- or a part of the wind farm can be treated as a power system with generation points, distribution net and delivery points (customers). A wind farm can also be modeled in simulation software, using a reverse power flow. In this case the wind turbines are simulated as loads and the normal delivery point as a generator. When performing this reverse power flow approach, the related customer indices can be utilized for analyzing the availability of the wind turbines.

When constructing a wind farm offshore, the work is very complicated and it is related to major investment costs which put high expectation on its possibility of delivering energy. The power delivered by the wind farm depends on many different aspects such as generation capacity, variations in wind, failure rate, outage time and so on. In the designing phase of a wind farm estimations and calculations are performed in order to evaluate how much energy it is likely to produce in average. The average energy production can then easily be converted into average expected income from the power plant. These numbers can then further be used in order to estimate the number of years to break even, i.e. when the wind farm will cover its investment cost. For these calculations the most relevant indice for analyzing the reliability of

the system is Energy Not Supplied (ENS) [MWh/year]. ENS is affected by both failure rate and outage time which reflects the reliability of a wind farm. The ENS-value is suitable in order to evaluate how much of the expected energy that will not be produced and supplied to the customers. It is also useful in comparing the benefits of reliability improvements in different wind farm topologies. The difference in the ENS-index can also be converted into economical benefits achieved by reliability improvements.

Energy Not Supplied (ENS) [MWh/year]:

$$ENS = \sum U_i L_{a,i} \quad (10)$$

where  $L_{a,i}$  is average load in MW connected to load point  $i$  and  $U_i$  is the unavailability of load point  $i$ .

### 2.3.4 Series and parallel systems

It is important to consider the topology of the power system; it can often be represented by series and parallel structures. When calculating the average failure rate, average outage time and average annual outage time of the system it is important to consider whether the components are connected in series, in parallel or both. One important part in reliability assessment is to analyze the impact of the possible failures that may occur in the system. The main focuses lay on detecting and clearing the abnormality of the system and apply corrective action such as removing the failed component or rescheduling the generation unit.

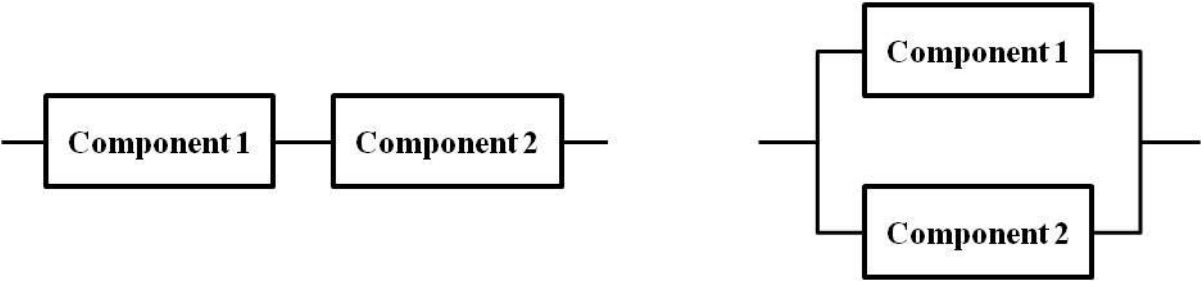


Figure 9. Two components connected either in series or parallel.

#### Series structure

Components in radial distribution systems are connected in series and it is of necessity that all the components operate simultaneously for the system to be in operating mode. For instance a

system with two series components requires functioning of both components in order to be available. For a radial distribution system, which is comparable to a collection grid of an offshore wind park, with  $i$  number of series components supplying load  $s$ , the related equations are defined in the following [6].

Average Failure Rate for Load [failure/year],

$$\lambda_s = \sum_i \lambda_i \quad (11)$$

Average Annual Outage Time for Component [hours/year],

$$U_i = \lambda_i r_i \quad (12)$$

Average Annual Outage Time for load [hours/year],

$$U_s = \sum_i \lambda_i r_i \quad (13)$$

Average Outage Time for Load [hours],

$$r_s = \frac{U_s}{\lambda_s} = \frac{\sum_i \lambda_i r_i}{\sum_i \lambda_i} \quad (14)$$

where subscript  $s$  denotes a system with series connected components.

### **Parallel structures**

When the system consists of parallel connected components, the function of one of the components is enough to keep the system in operation mode. This fact is given that the transmission line can handle the extra load and fulfill the N-1 criterion. All components must be out of service at the same time to cause a system failure.

For second-order events, a parallel reliability system with two components connected in parallel. The equations for average failure rate, average outage time and average annual outage time of the system are defined in the following [1].

$$\lambda_p = \frac{\lambda_1 \lambda_2 (r_1 + r_2)}{1 + \lambda_1 r_1 + \lambda_2 r_2} \quad (15)$$

$$r_p = \frac{r_1 r_2}{r_1 + r_2} \quad (16)$$

$$U_p = \lambda_p r_p = \lambda_1 \lambda_2 r_1 r_2 \quad (17)$$

where subscript p denotes a system with parallel connected components.

## CHAPTER 3: NEPLAN

---

*NEPLAN is a software which will be used in this project in order to evaluate different topologies of a wind farm. The software is suitable for this purpose as it can handle reliability calculations with the load considering constraints on the cable capacity.*

---

### 3.1 NEPLAN Planning and Optimization Software

NEPLAN is planning and optimization software for electrical, heat, gas and water networks which has been developed by the BCP group in Switzerland. It is used to analyze, plan, optimize and manage power networks which includes optimal power flow, transient stability and reliability analysis. The software package can be used for transmission and distribution system analysis and the reliability software can provide reliability indices for individual load points and the overall power system. It can also provide information based on the cost of unreliability along with investment analysis and the Net Present Value (NPV) of different investment alternatives. NEPLAN uses the homogenous Markov process for the calculations and it handles up to second order contingencies. The NEPLAN tool is very flexible and user friendly planning tool where network designers can compile different topologies. [3], [4].

### 3.2 Fundamental Calculation Flow in NEPLAN

NEPLAN as a reliability analysis tool is based on the Markov method which is briefly explained in previous chapter. The fundamental calculation flow in NEPLAN can be visualized as in figure 6. The output of this evaluation approach is reliability indices for both load point and the overall system along with load flow constraints [4].

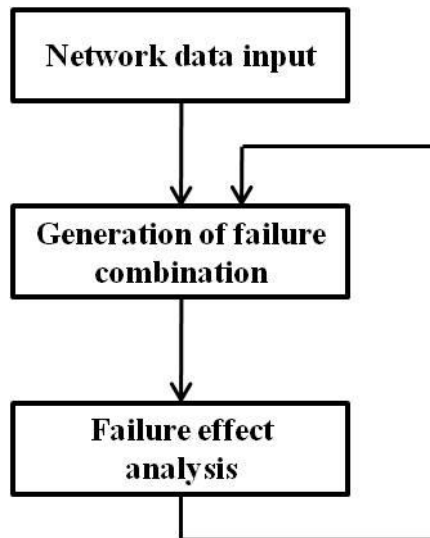


**Figure 10. Fundamental Calculation Flow in NEPLAN [4]**

### **3.2.1 Network data input**

Some data needed for the calculations are active (P) - and reactive (Q) power at generation and load points, failure rate ( $\lambda$ ), failure duration time etc. These data are implemented in the model and the topology can be analyzed in its normal conditions. Besides these data a reference bus must also be defined.

There are typically three levels of input for reliability data which consider overall system defaults, defaults per substation and data for individual components. Further NEPLAN consider five different types of reliability data i.e. component, line, switch, generation unit and load [4].

### **3.2.2 Generation of failure combination**

The next step is to analyze the system behavior in case of failure. By doing this it requires extensive knowledge and understanding on the practical system. The network will be exposed to different possible scenarios by applying the contingency screening and ranking technique [1]. By using the network reduction technique it would be possible to accelerate the calculations. Where the objective of contingency screening and ranking function is to shortlist a specified number of critical contingencies from a large list of credible contingencies and rank them according to their severity.

The predefined outage events in NEPLAN are divided in two groups and defined as first- and second order contingencies. The first order contingencies deal with single stochastic- and

single deterministic outages while the second order contingencies can be considered either as two stochastic- or stochastic and deterministic outages.

The different failure combinations can consist of single stochastic outages, overlap of two stochastic outages or overlap of one stochastic and one deterministic outage.

Single stochastic outages can consist of single independent- or common mode outage, ground fault or unintended switch opening. The reliability input data for these categories are failure rate and repair time, the output data are failure frequency and its relevant duration.

Second order contingencies can be considered either as two stochastic outages or stochastic and deterministic outages.

### **3.2.3 Overlapping stochastic outages**

Independent outages can occur at the same time and overlap one and another. They are then called overlapping stochastic outages and can consist of numerous different combinations like [4]:

- multiple independent failures
- single independent failure plus manual disconnection
- single independent failure plus common mode failure
- single independent failure plus line-to-ground fault
- multiple manual disconnections
- manual disconnection plus common mode failure
- manual disconnection plus line-to-ground fault
- multiple common mode failures
- common mode failure plus line-to-ground fault

The occurrence of overlapping outages can be graphically visualized as in Figure 11.

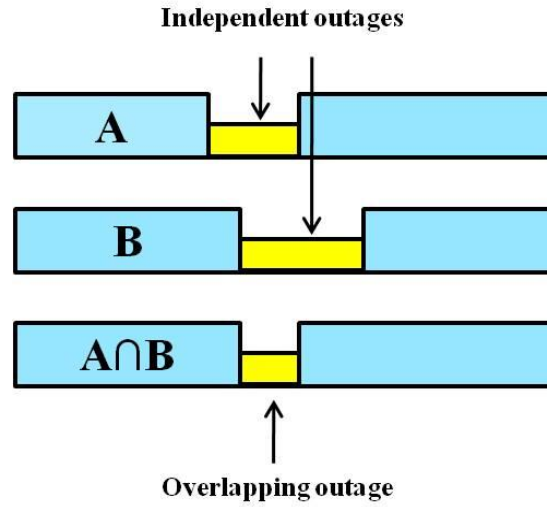


Figure 11. Overlapping stochastic outages [4]

In the case of overlapping of two stochastic outages, named A and B, the failure frequency can be obtained from the homogenous Markov process [1].

$$FF = \lambda_A \lambda_B (r_A + r_B) \quad (18)$$

where  $\lambda_A$  and  $\lambda_B$  are the failure rate and  $r_i$  is their relevant repair time.

In the case where the second outage is a consequence of the first one, they are said to be dependent and the second outage may occur with the probability Pr. This can be the case with multiple ground faults due to increased voltage during the first, which may lead to second short circuit. Another case is when protection fail to trip or trip unwanted due to faulty protection settings. For dependent outages the failure frequency can be calculated as [1].

$$FF = \lambda_A Pr_B \quad (19)$$

Deterministic outage, like preventive maintenance, do by itself not cause load supply interruptions in the system. When though deterministic and stochastic outages occur at the same time it may lead to forced outage and load failure. The processing of such overlapping outages proceeds in the same way as single stochastic outages. The failure frequency at load points can be calculated as [1].

$$FF = \lambda_A \lambda_B r_B \quad (20)$$

where  $\lambda_A$  and  $\lambda_B$  are the failure rate for stochastic and deterministic outages respectively and  $r_i$  is their relevant repair time for maintenance.

### 3.2.4 Failure effect analysis

The final step includes evaluation of the effect contributed by possible failure outcomes. All the possible failures are registered and the relevant indices associated to each load points and the overall network is calculated. In this step the effects of load flow and the need for load shedding is also presented by NEPLAN. The reliability indices which are provided by NEPLAN is shown in Table 1 for individual load points and in

Table 2 for the overall power system.

**Table 1. Load point indices [4], [5]**

Index	Unit	Description
Interruption Frequency	[1 /yr]	Expected frequency of supply interruption per year
Interruption Duration	[min/ yr] [hrs/ yr]	Expected probability of interruption in minute or hours per year
Mean Time of interruption	[min,hrs]	Average duration of customer interruption
Power not supplied	[kW/ yr] [MW/ yr]	Product of interrupted power and its interruption frequency
Energy not supplied	[kWh/ yr] [MWh/ yr]	Product of interrupted power and its interruption probability
Interrupted cost	[\$/ yr]	Cost of supply interruption

**Table 2. Overall system indices [4], [5]**

Index	Unit	Description
N	-	Total number of customers served
SAIFI	[1/ yr]	System average interruption frequency index
SAIDI	[min/yr]	System average interruption index
CAIDI	[h]	Customer average interruption duration index
ASAI	[%]	System average availability index
F	[1/ yr]	System load interruption frequency
T	[h]	System load interruption frequency
Q	[min/ yr]	System load interruption probability
P	[MW/ yr]	Total interrupted load power
W (ENS)	[MWh/ yr]	Total load energy not supplied
C	[CU/ yr]	Total load interruption cost

### 3.3 Example cases with NEPLAN and analytical calculations without considering load flow

The aim of this section is to provide basic understanding of how NEPLAN executes its calculations. This is carried out by; Building a simple network model in NEPLAN and apply manual hand calculations in order to obtain load point indices and clarify the reliability calculation approach. The objective is also to demonstrate how the software calculates the indices. Calculations will be performed on series- and combined series and parallel networks.

This procedure is suitable while working with complex systems like a wind power system. In order to execute a proper analysis of such systems a certain level of modeling has to be made. When modeling a complicated system, a good approach is to divide the system into smaller parts such as subsystems or components.

To begin with calculations are performed on a simple radial network using series component equations 11 and 14 in order to calculate the failure frequency and its related duration.

The input data used for the network model is presented in following tables.

**Table 3. Elements reliability data**

Elements	Failure rate	Duration [hour]
Busbar	0.001	2.0
Circuit breaker	0.02	24
Transformer	0.015	15
Disconnecting switch	0.002	4.0

**Table 4. Load data**

Load point	Number of customers	Active power	Reactive power
Load 1	80	400 MW	200 MVar
Load 2	100	400 MW	200 MVar

#### 3.3.1 Radial network calculations

Figure 12 shows the basic radial network modeled in NEPLAN utilized for the first reliability calculations. Figure 11 and 12 are an exact replica of how it looks in NEPLAN.

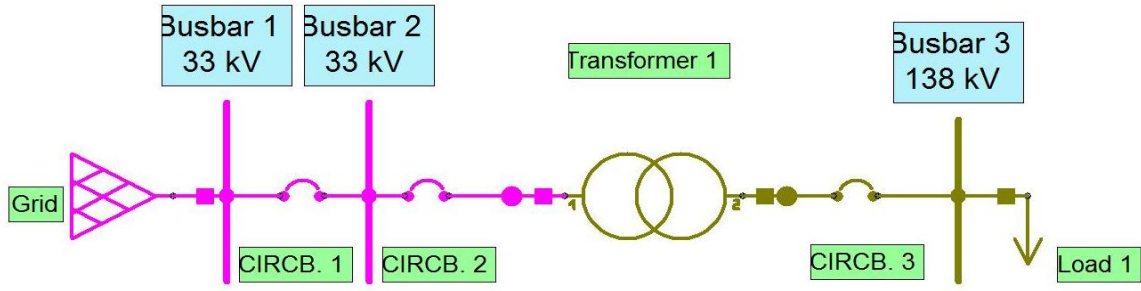


Figure 12. Radial network

Hand calculation of Load point indices for Load 1:

$$FF = \lambda_{BB1} + \lambda_{CB1} + \lambda_{CB2} + \lambda_{TR1} + \lambda_{CB3} + \lambda_{BB3} + \lambda_{LP1}$$

$$FF = 0.001 + 0.02 + 0.001 + 0.02 + 0.015 + 0.02 + 0.001$$

$$FF = 0.078 \left[ \frac{1}{year} \right]$$

Failure duration calculation for load point 1:

$$r_s = \frac{\sum_i \lambda_i r_i}{\sum_i \lambda_i}$$

$$r_s = \frac{0.001 * 2 + 0.02 * 24 + 0.001 * 2 + 0.02 * 24 + 0.015 * 15 + 0.02 * 24 + 0.001 * 2}{0.078}$$

$$r_s = 21.423 \left[ \frac{hours}{year} \right]$$

System indices are calculated for load point 1, using equations 6-9:

$$SAIFI = \frac{0.078 * 80}{80} = 0.078 \left[ \frac{int.}{yr, cust.} \right]$$

$$SAIDI = \frac{0.078 * 21.423 * 80 * 60}{80} = 100.260 \left[ \frac{min}{yr, cust.} \right]$$

$$CAIDI = \frac{0.078 * 21.423 * 80}{0.078 * 80} = 21.423 [h]$$

$$ASAI = \frac{(80 * 8760) - (0.078 * 21.423 * 80)}{80 * 8760} * 100 = 99.981 \text{ [%]}$$

**Comparing hand calculations with results obtained from NEPLAN for the radial system:**

Load point indices for radial network:

**Table 5. Load point indices for system illustrated in Figure 12.**

Load Point	Failure Frequency [1/year]		Failure Duration [h]	
	Hand	NEPLAN	Hand	NEPLAN
Results obtained by:				
Load 1	0.078	0.078	21.423	21.425

Overall system indices for radial network:

**Table 6. Overall system indices for the system illustrated in Figure 12.**

Results obtained by:		Hand	NEPLAN
Index	Unit	Value	Value
N	-	80	80
SAIFI	[1 yr]	0.078	0.078
SAIDI	[min yr]	100.260	100.253
CAIDI	[h]	21.423	21.425
ASAI	[%]	99.981	99.981

### 3.3.2 Combination of series and parallel network calculations

In the next step, calculations are performed on a simple network which consists partially of series- and parallel connected components. Because of the protection system in forms of circuit breakers installed before and after the transformers, this section cannot be treated as a parallel circuit when performing the calculations. With this protection setup, one of the transformers can continue to run in case of failure in the other one. Thus the transformers do not contribute to the failure frequency and its related duration. The installed circuit breakers should though be included in the calculations. This protection setup is preferable in case of reducing load interruptions. In this case it is possible to perform maintenance in one of the transformers without causing any load interruptions.

Figure 13 shows the combination of series and parallel network which is utilized for the second reliability calculations.

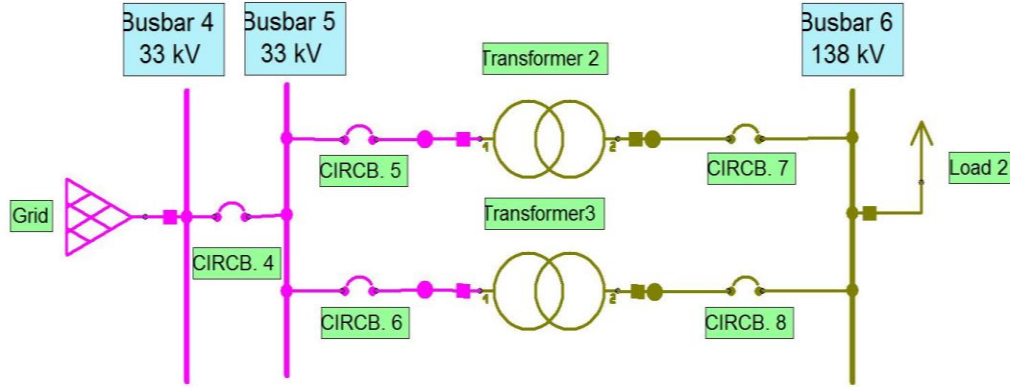


Figure 13. Combination of series and parallel network

$$FF = \lambda_{BB4} + \lambda_{CB4} + [\lambda_{CB5} + \lambda_{CB6} + \lambda_{CB7} + \lambda_{CB8}] + \lambda_{BB6} + \lambda_{LP2}$$

$$FF = 0.001 + 0.02 + 0.001 + [4 * 0.02] + 0.001$$

$$FF = 0.103 \left[ \frac{1}{year} \right]$$

$$r_p = \frac{0.001 * 2 + 0.02 * 24 + 0.001 * 2 + [4 * (0.02 * 24)] + 0.001 * 2}{0.103}$$

$$r_p = 23.359 \left[ \frac{hours}{year} \right]$$

System indices are calculated for load point 2, using equations 6-9:

$$SAIFI = \frac{0.103 * 100}{100} = 0.103 \left[ \frac{int.}{yr, cust.} \right]$$

$$SAIDI = \frac{0.103 * 23.359 * 100 * 60}{100} = 144.359 \left[ \frac{min}{yr, cust.} \right]$$

$$CAIDI = \frac{0.103 * 23.359 * 100}{0.103 * 100} = 23.359 [h]$$

$$ASAI = \frac{(100 * 8760) - (0.103 * 23.359 * 100)}{100 * 8760} * 100 = 99.973 [\%]$$

**Comparing hand calculations with results obtained from NEPLAN for combined network:**

Load point indices for the combination of series and parallel network:

**Table 7. Load point indices for system illustrated in Figure 13.**

Load Point	Failure Frequency [1/year]		Failure Duration [h]	
	Hand	NEPLAN	Hand	NEPLAN
Load 2	0.103	0.103	23.359	23.362

Overall system indices for the combination of series and parallel network:

**Table 8. Overall system indices for the system illustrated in Figure 13.**

Results by:		Hand	NEPLAN
Index	Unit	Value	Value
N	-	100	100
SAIFI	[1/yr]	0.103	0.103
SAIDI	[min/yr]	144.359	144.344
CAIDI	<i>h</i>	23.359	23.362
ASAI	%	99.973	99.973

## CHAPTER 4: Offshore wind farm grid topology

---

*The aim of this chapter is to illustrate the current state of the art in grid configuration of offshore wind farms.*

---

### 4.1 Different layouts for offshore collector systems/Common grid topology structures

There are different arrangements for wind farm collector systems and the grid can be designed for AC, DC or both AC and DC. The study performed in this report does however only consider AC transmission with a collector voltage of 33 kV. Cables are buried at a depth of 1,5-2m under the seabed to protect the cables from external damages. These conditions makes that repair of cables can be difficult and long, especially if cable vessels necessary to the work, are not available.

Most operational offshore wind farms have radial internal array grid connection topologies. An exception is North Hoyle [17] and some more recent projects, such as the Alpha Ventus [27] and Great Gabbard [28] which also includes redundancy. This may suggest that electrical grid designer have identified these topologies advantageous. The radial topology has however been reconsidered for upcoming wind farms and including redundancy, like North Hoyle, has become a topic. Alternative designs and possible future designs are discussed in the following sections.

The electrical system for an offshore wind farm concerns all those components that enable the integration of the wind turbine to the grid supply point. Examples of such components are generating units, switchgear, transformers, inter turbines and transmission cables, power electronic converters etcetera. The overall function of the electrical system is to collect power from each wind turbines, to transmit the power to shore and to convert it to appropriate grid voltage and frequency. When designing the overall wind farm the aim is to minimize the energy cost by balancing the overall wind production, (- taking into account the distribution of wind speed and direction as well as the turbulence between turbines (wake effect), bathymetry and geotechnical conditions), and investment and operational costs.

There have been several studies performed in evaluating different layouts for offshore collector systems. There is a project called Downvind (Distant Offshore Wind farms with No Visual Impact in Deepwater) where a project group studied and evaluated the offshore grid of offshore wind farms. In this study, four different conceptual designs have been identified [18]:

- Radial design, where all wind turbines are connected to a single cable feeder within a string.
- Single-sided ring design, where a redundant path is included for the power flow within a string.
- Double-sided ring design, where redundancy is provided by the establishment of a looped circuit between the wind turbines.
- Star design, where the wind turbines are distributed over several feeders, allowing the use of lower rated equipment.

The options may all be utilized for both AC and DC solutions. These four design options are presented in the following along with two additional alternatives.

#### **4.1.1 Radial design**

Figure 14 shows the layout of a radial offshore grid where the wind turbines are connected to a single cable feeder within a string and collected at the collector hub. The maximum number of wind turbines that can be connected to each string feeder is determined by the subsea cable ratings and the capacity of the generator. This design is simple to control but the main advantage is the relatively low cable costs due to the possibility of taper the cable ratings between the turbines. This is possible because with increased distance from the hub and decreasing numbers of turbines connected in series, the amount of power transmitted is smaller further out in each feeder. The major disadvantage with this design is the comparatively poor reliability. Cable or switchgear faults at the hub side of the feeder will lead to the loss of power from all downstream turbines in the feeder [18], [14].

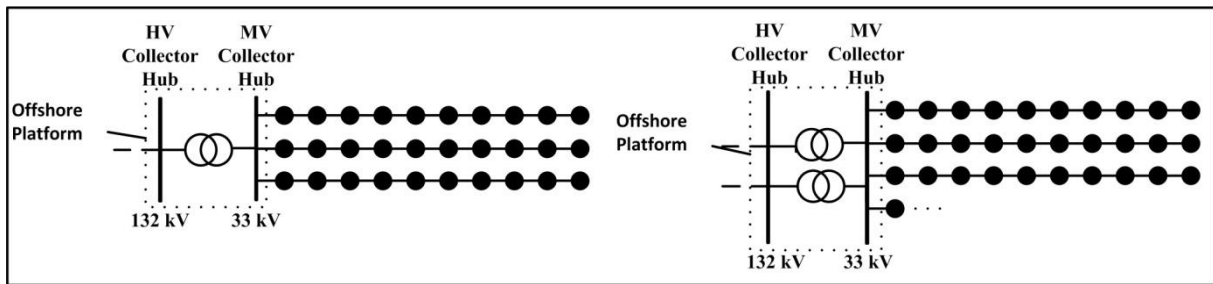


Figure 14. Radial design with one and two feeder cables to shore

#### 4.1.2 Single-sided ring and shared ring design

Figure 15 shows the single-sided ring design. This design has additional parallel cables for each string, forming a looped design. Comparing to the radial design this alternative addresses some of the reliability issues by providing a redundant path for the power flow within a string. In the single-sided ring design, this additional security comes at the expense of higher cable costs due to the extra cable. This cable is installed from the collector hub to the last turbine in the string with the switching device normally opened. This implies that in case of a fault between the collector hub and the first turbine, it is not possible to taper the cable ratings because the ringed path must be able to carry the entire power flow of all turbines. Despite the increase in cable costs compared to the radial system, an initial feasibility commissioned by the DOWNVIInD consortium recommended and utilized this design for the studied 1 GW offshore wind [18], [14].

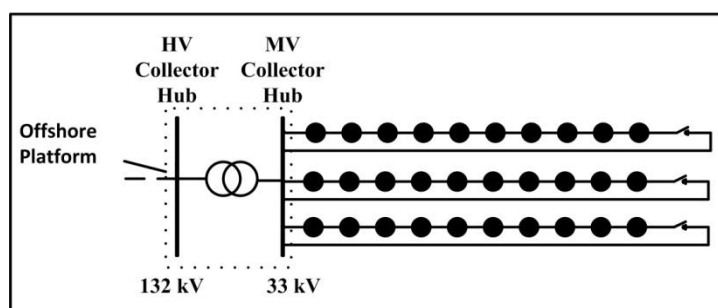


Figure 15. Single sided ring design

#### 4.1.3 Double-sided ring

Figure 16 shows the double sided ring, which is another version of a looped design. Two strings are connected in parallel in order to provide redundancy. For this design solution the

cable length for the two strings will only increase by the distance between the turbines at the end of the strings. Like for the single-sided ring design tapering of the cable ratings is maybe not an alternative because all cables should be able to handle the full power flow of the extra transmission in one string in case of fault. The cables ratings can be tapered and load shedding can be performed in case of overload. This is however an economical issue, where the extra installation costs must be weighed against the expected value of lost load over the lifetime of the wind farm [18], [14].

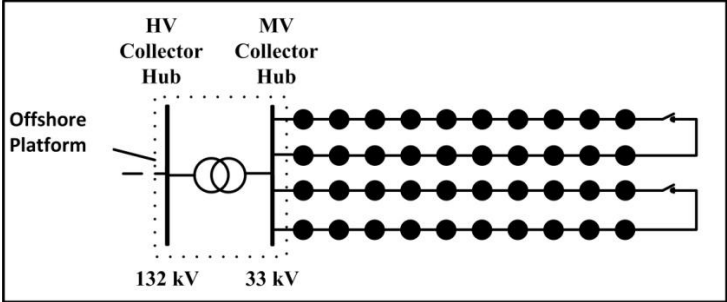


Figure 16. Double-sided ring

4.1.4 Star design

Figure 17 shows the star design. In this design the cable ratings can be low and it can provide a high level of security for the wind farm as a whole. In case of a cable outage, this will only affect one wind turbine, except for the case when a fault occurs in the feeder cable to the hub. Another advantage for this design is that the voltage regulation along the cables is likely to be better. The downside for the star design is the increased expenses due to the longer diagonal cable runs and the short section of the higher rated connection to the hub. The major cost implication of this option is the more complex switchgear requirement at the central turbine of the star [18], [14]Error! Reference source not found..

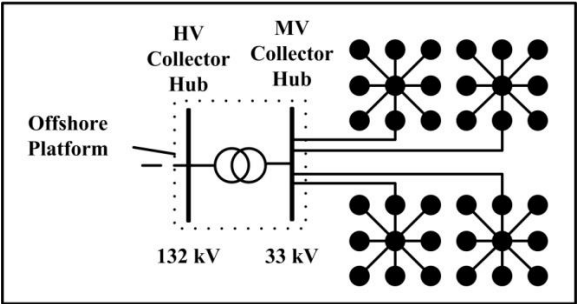
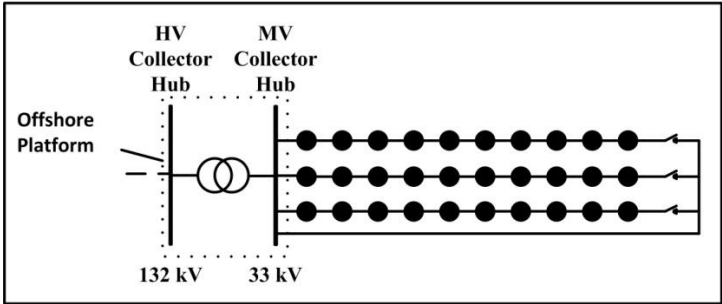


Figure 17. Star- or cluster design

**4.1.5 Single return- or shared ring design**

Figure 18 shows the design option single return- or shared ring design. This design consists of a number of strings connected in parallel with a redundant cable. The redundant circuit is designed to potentially deliver the full power output of a failing string within the arrangement. The probability of two or more feeders failing at the same time is considered to be relatively small and the redundant cable is dimensioned handle the load of one string only.



**Figure 18. Single return- or shared ring design**

**4.1.6 Double-sided half-ring design**

Figure 19 shows the double sided half-ring design which is a semi variant of the double sided ring design. This is a configuration which could be interesting in case when little modifications are covered compared to the radial design. This layout can isolate five turbines in case of a cable failure in the beginning of an array and provide an extra path for the remaining five turbines. This layout should also include remote controlled load switches booth in each array and the loop. In this way it is possible to remotely isolate five turbines at the time.

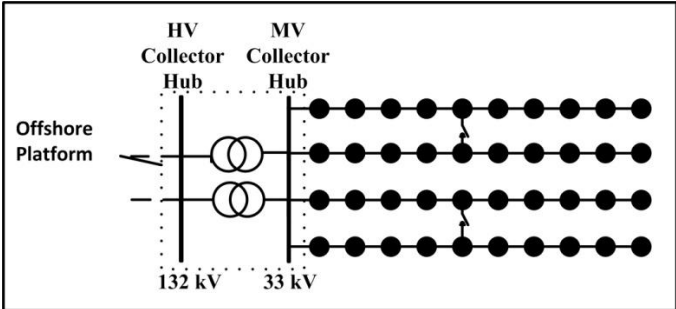


**Figure 19. Double-sided half-ring design**

## 4.2 Thanet offshore wind farm

In this section the grid topology of the Thanet offshore wind farm is presented for illustration, and as a basis for creating a topology base case. The 300 MW wind farm is currently the largest offshore wind farm operating and it has been selected for this reason as representative of the current state of the art in grid topology.

### 4.2.1 Basic information and location

The Thanet Offshore Wind Farm is owned by Vattenfall and the construction of the wind farm was commissioned in September 2010. The total investment for completing the wind farm is in the order of around £780 million. The wind farm consists of 100 Vestas V90 3 MW turbines which gives a total capacity of 300 MW. The wind farm covers an area of 35 square kilometers and is located approximately 12 kilometers north east of Foreness Point, the eastern tip of Kent. The onshore power substation is located in Richborough [20], [21].



Figure 20. Location of the Thanet offshore wind farm. [22]

Each wind turbine sits atop a steel monopole foundation at a water depth between 20 and 25 meters. The tower of the wind turbines is connected to the foundation by a transition piece. The hub of the wind turbine is located at 70 m height above sea level. The wind farm consists of seven rows where the distance between turbines is approximately 500 meters along the rows and 800 meters between the rows. The inter-array cables interconnect the wind turbines within the arrays to each other and to the offshore transformer substations. The cables are standard 3-core, copper conductor, cross-linked polyethylene (XLPE) insulated and armoured submarine cable, rated at 33 kV.

The output from the turbines is fed to an offshore substation composed of two 180 MVA power transformers that increase the voltage from 33 kV to 132 kV. The substations will also include high-voltage and medium-voltage switchgear with the necessary protection and control technology. There is also an auxiliary system with emergency power supply on the platform.

Two three-phase 132 kV high-voltage subsea cables are transporting the electrical power from the offshore substation to the onshore grid connection point, a new high-voltage switching station in Richborough, Kent. The substation, which will act as the grid connection point on the coast, has a system for reactive-power compensation based on SVC (Static Var Compensator) technology. The reactive-power compensation system fully meets the requirements of the British power supply system (National Grid Code). It provides the necessary power factor correction and improves the voltage quality [20], [21].

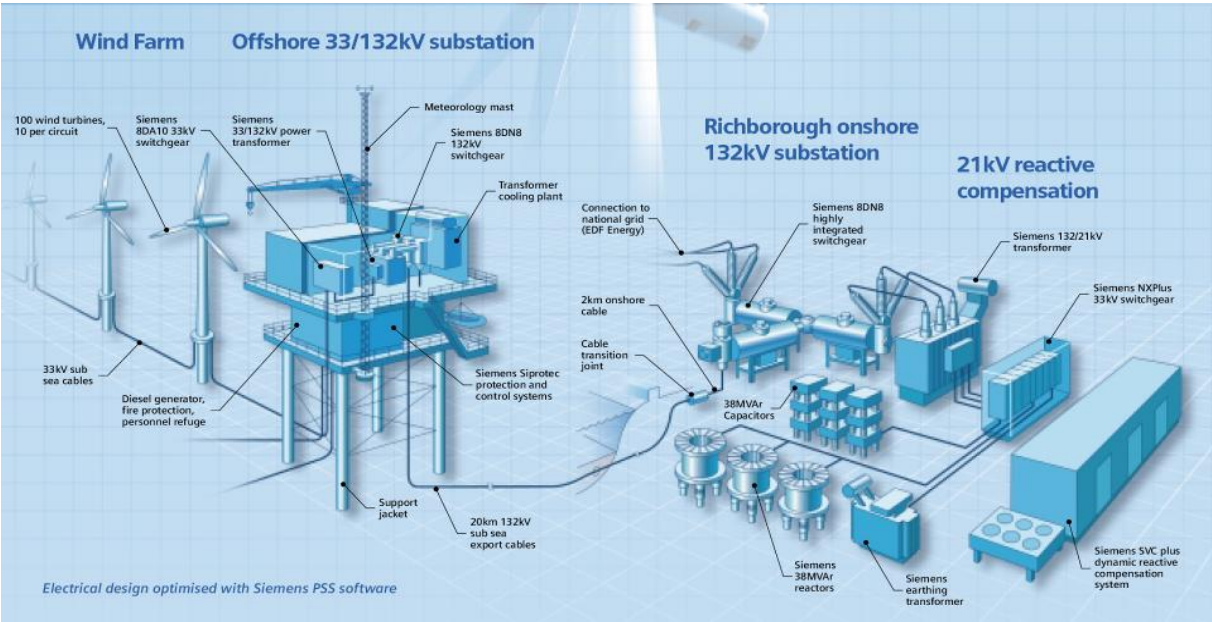
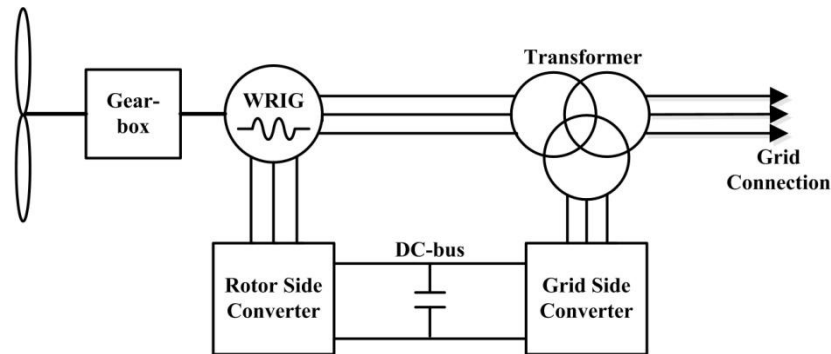


Figure 21. Grid connection for the Thanet offshore wind farm [22].

4.2.2 Turbines technical specifications

The Vestas V90 3 MW turbine is a three bladed upwind wind turbine generator that uses pitch control for variable speed. It has a 4-pole Double Fed Induction Generator with a rated voltage of 1000/400 V AC at 50 Hz. The turbine delivers the energy via a gearbox with two

planetary stages and one helical stage. Inside the nacelle there is a transformer which steps up the voltage level from the generator voltage of 1000/400 V AC to 33 kV. Each turbine is connected to the 33 kV internal network through a switchgear in every tower consisting of a remotely controlled circuit breaker and disconnecting switch [20], [21], [13].



**Figure 22. General Configuration of a Doubly Fed Induction Generator (DFIG), which is the name of the complete Wound Rotor Induction Generator (WRIG)/converter system [25].**

#### 4.2.3 Internal networks technical specifications

The wind farm consists of seven rows with the offshore platform situated in the center. There are ten array cables connected to the platform each with ten turbines interconnected with a radial configuration (see Figure 23). The submarine cable used for the inter array network is a XLPE insulated 3-core copper conductor rated at 33 kV. The area of the copper conductor depends on the power flow and how many turbines which are followed by the connection point in the string. Another limitation factor to consider when dimensioning the cables is the increased heat due to less cooling inside the J-tube within the foundations and the cables are also buried 1,5-2m under the seabed. Due to this reason the rating of the cable is generally increased by 10-12 %. There are three different cable cross sections often used for the inter array connections which are 400 mm<sup>2</sup>, 300 mm<sup>2</sup> and 95 mm<sup>2</sup>. The distribution of the cable dimensions can be observed in Figure 22 [20], [21], [13].

## Thanet wind farm layout

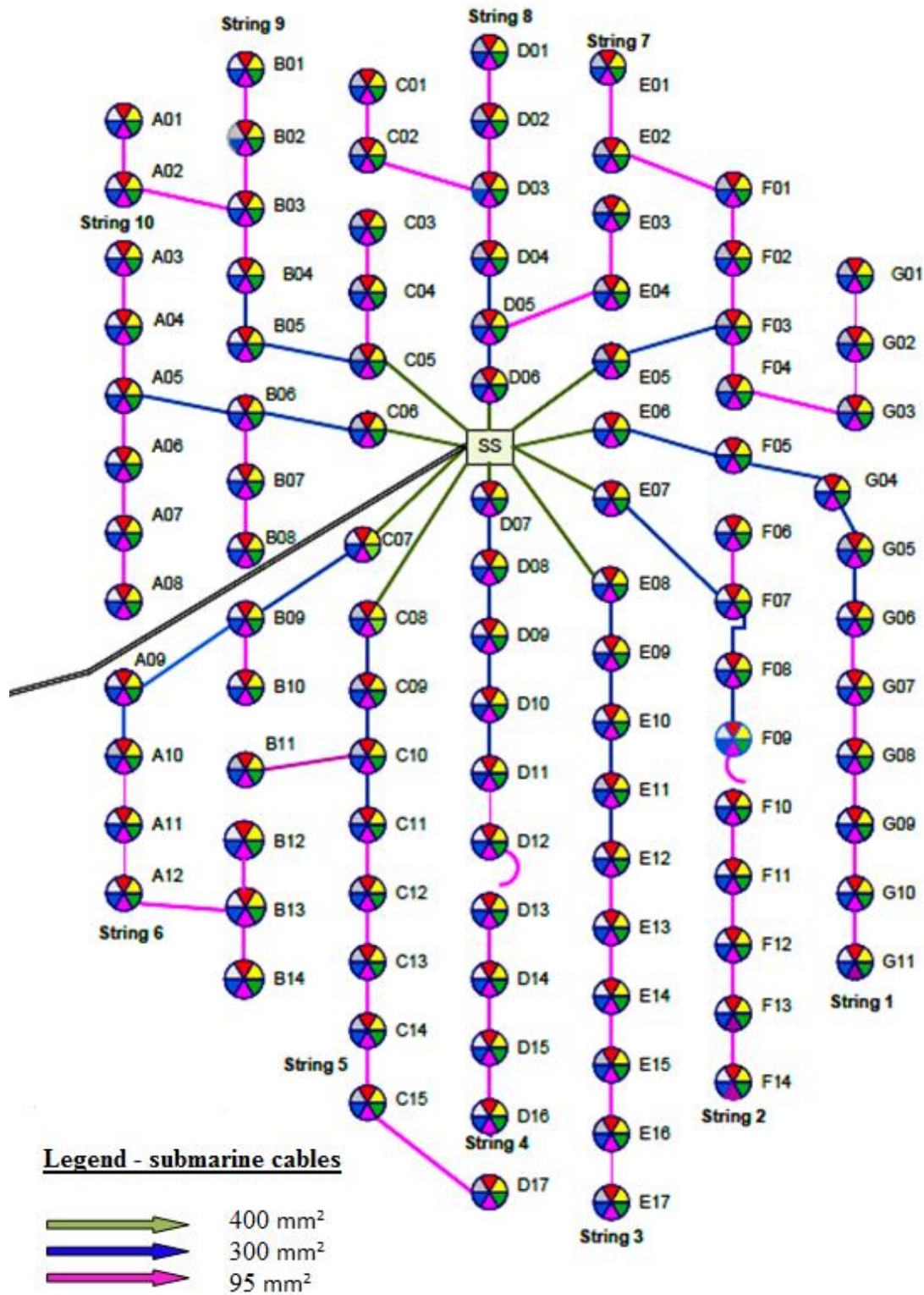


Figure 23 – Layout of the Thanet wind farm. It is composed of ten array cables connecting one hundred 3 MW turbines to an offshore substation. At the substation, two 180 MVA transformers increase the voltage from 33 kV to 132 kV. The electrical power is then transmitted to the onshore grid connection point in Richborough by two three-phase 132 kV subsea cables [20].

# CHAPTER 5: Analysis of different topologies

*This chapter presents the data used for the models and the different topologies chosen for the analysis are presented. Some drawbacks and benefits are also discussed for each topology.*

The software NEPLAN is used in order to analyze power flow and reliability of different topologies. For the study the distribution generators in the wind turbines are modeled and represented as loads using a reverse power flow approach. The reason for this approach is to be able to model the possibility to control the output power of the wind turbines, which was not possible in NEPLAN for a generator. This is done for each load point (each wind turbine) by allowing complete load (production) shedding. All the cables are modeled as pi-equivalents in NEPLAN, working in steady state conditions. Parameters used for modeling the cables, in addition to the reliability data, are: resistance R, inductance X, capacitance C and the maximum current- and voltage ratings for the cable. The cable lengths and distances between turbines and platform can be seen in Figure 24.

In the original topology along with the alternative topologies, there are different protections elements like: circuit breakers, load switches and disconnectors included. These devices are considered correctly dimensioned and treated as ideal elements during the load flow analysis. For the reliability analysis, these elements are though of considerable importance because of their contribution of the overall performance of the system. The reliability data used for modeling are based on [6] and [10], with supplements from [26], and are presented in Table 9.

**Table 9. Reliability data**

Component	Failure rate [failure/year]	Repair time [hours]	Switching time [min]
Subsea cables (33 kV)	0.004	672	-
Disconnectors (33 kV in wind turbines) (Manual)	0.01	120	10080*
Circuit breakers (33 kV on offshore platform)	0.03	120	20
Load switches (33 kV in wind turbines)	0.01	120	20

**\*One week switching time including isolation of the fault. Switching has to be performed by service personal going to the turbine by boat.**

When studying the different topologies and evaluating the change in performance on different layouts, the only interesting parameters are: different cable ratings and reliability data for cables and switching devices. Thus the wind turbines (bus and load) and the offshore platform (bus and generator) are considered as ideal elements. For this study, voltage drop in the system is neglected because this is considered rather easy to avoid and can be compensated with reactive power in the reality. The cable loops which are included in some of the topologies are modeled as ideal elements considering that faults occur rather seldom and that the loops are not included in the regular performance of the network.

A wind farm is a very intermittent energy resource and the power production varies considerably over time. Because of this it would not provide a fair comparison between the different topology options if they only where modeled on maximum production level. In case of failure the different topologies provides alternative paths for the power to flow, with different power ratings. This fact contributes to different abilities of producing electricity during fault compared to alternative layouts. In order to create a more realistic power production scenario for each topology, the power production is divided in four different production levels. Each level is based on the wind probability density function at the production site, combined with the power curve of the Vestas V90 3 MW wind turbine. The production level for each case is provided in Table 10.

**Table 10. Production level for each case**

Case	Wind speed [m/s]	Avg. production [MW]	Probability [%]
1	0-3	0	14
2	4-8	0,425	45
3	9-12	1,834	26,5
4	13-25	2,947	14,5

The average annual electricity generation in one year on the Thanet wind farm is 960 GWh. [23] which corresponds to a capacity factor of 36,53%.

The ENS values for each case and topology are weighted with the probability for each case and a mean value of ENS is presented in order to compare each topology. The calculations are performed in Excel and only the ENS mean value is presented for each topology.

Cost data used in the study for investment analysis and evaluation whether a change in layout could be financially beneficial or not, are collected from [10] and [24]. The data used for investment analysis are presented in Table 11.

**Table 11. Cost data used for investment analysis.**

Discount rate	7 %
Expected income per MWh	0,18 [€/MWh]*
Expected lifetime of the wind farm	20 [years]
Vessel and installation cost, cable	200 [k€/km]
Load switch with V, I measurement	10 [k€]
<b>Cable dimensions [mm<sup>2</sup>]</b>	<b>Cost [k€/km]**</b>
95	100
120	110
150	140
185	160
240	180
300	220
400	240
500	270
630	300
800	350
1000	360
1200	370

**\*Including electricity price and green certificates, valid 2010 in UK [24]. No predictions of future changes and inflation rates are taken into account.**

**\*\*Cable costs are collected from [10] for cable ratings up to 400 mm<sup>2</sup> and an extrapolation of the costs is performed for the remaining cable ratings.**

### **Alternative layout, Top.1**

Top.1 is the original topology of two branches on the Thanet wind farm which is used as a benchmark for evaluation of different topologies. Each row consists of ten 3 MW turbines with manual disconnectors situated in each tower and a voltage level of 33 kV. Each row of turbines is terminated with a circuit breaker on the offshore platform which is pictured as a bus to the left. The cables which are used to interconnect the turbines are three core armoured 33 kV XLPE copper cables.

In case of a fault on one of the cables the entire row is disconnected. The entire row with turbines will be disconnected and not be able to produce any electricity until the fault is identified and the affected cables and turbines are manually disconnected. This operation can take rather long time depending on the prevailing weather conditions.

If a fault is located in one of the turbines, this turbine can be remotely disconnected with the circuit breaker situated inside the turbine. In this way the remaining turbines can continue to operate after the turbine which is out of order is disconnected.

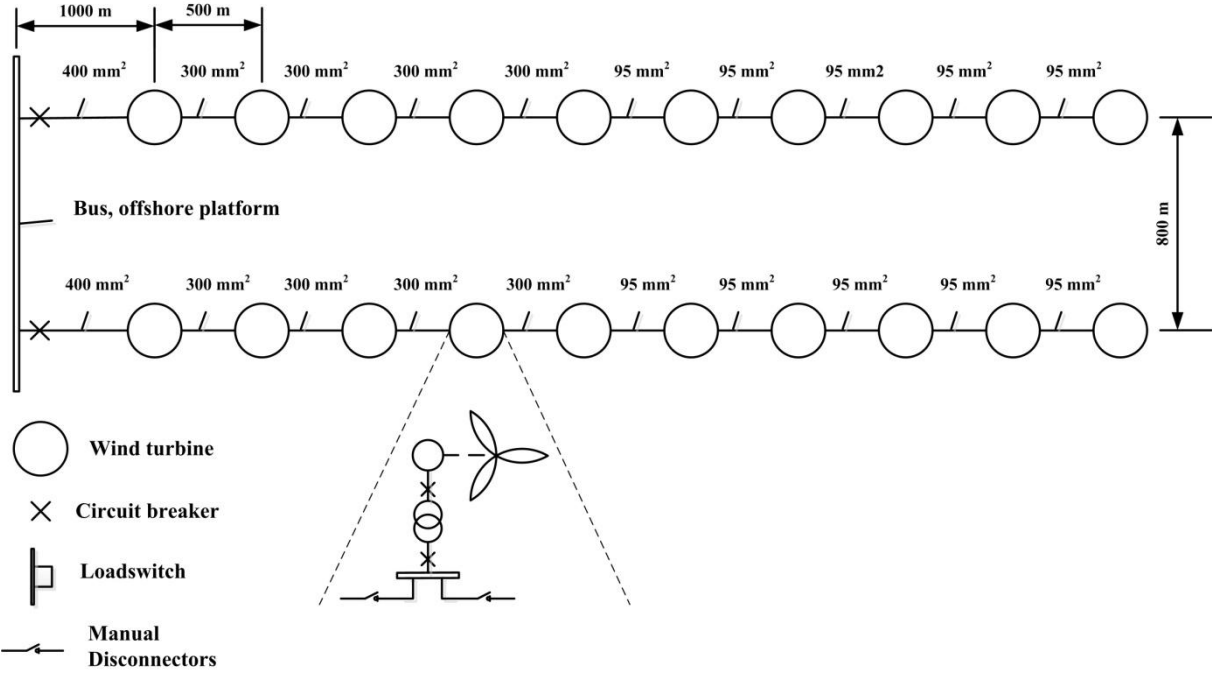


Figure 24. Original layout, Top.1,  $ENS = 810 \frac{MWh}{yr}$

**Alternative layout, Top.2**

Top.2 is the first alternative layout which is analyzed. This layout is the same as the original but a cable loop with a, normally open, remote controlled loadswitch is included in the end which connect the two rows to each other. A fault must be manually detected and isolated but this alternative can provide an extra path for the power to flow. In this layout the cables are though not dimensioned to bear any extra load besides the ten turbines at full load. This makes this layout not able to be fully utilized during strong winds and load shedding must be performed in order to not overload the cables. Load shedding can be performed remotely by turning the blades on the turbines. One should also consider that the average power production is around 37 % of full load which makes this solution useful in normal

conditions. The load will be limited in case of fault but the layout can overall deliver more energy with this alternative path for the load flow than without.

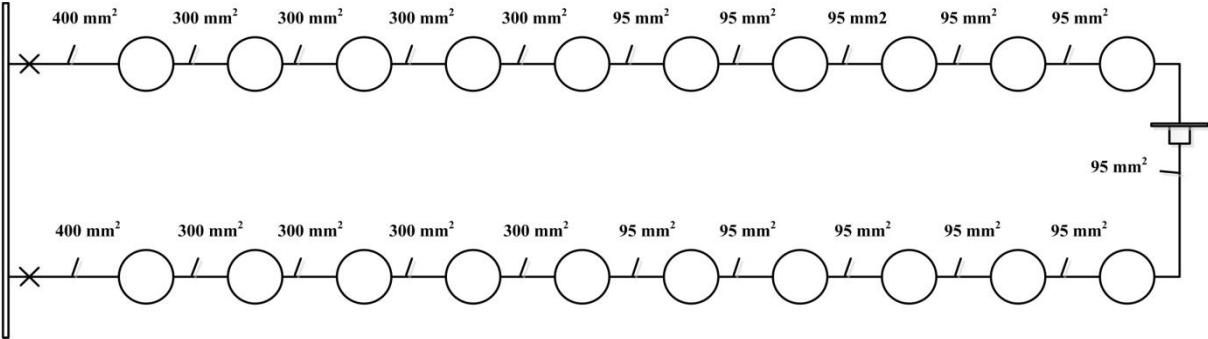


Figure 25. Top.2.  $ENS = 745 \frac{MWh}{yr}$

**Alternative layout, Top.3**

The layout of Top.3 is similar to Top.2 but two disconnectors are replaced by remote controlled load switches, which are included in the middle of each row. The two load switches on the row should be equipped with voltage and current measuring systems in order to be able to locate the failure remotely by analyzing these signals. Once located, a fault can be remotely isolated in each of the sections including five turbines. The energy produced by the five turbines which are not affected by the fault can then be transferred by the original- or the alternative path, depending on affected section. More load switches could be included in order to create more sections which could be remotely isolated in case of fault. With experience gained from previous studies [6] this is not a very good option due to; too many load switches including control systems will create complexity, without much gain in reliability. Because of that no topology with more load switches included are investigated.

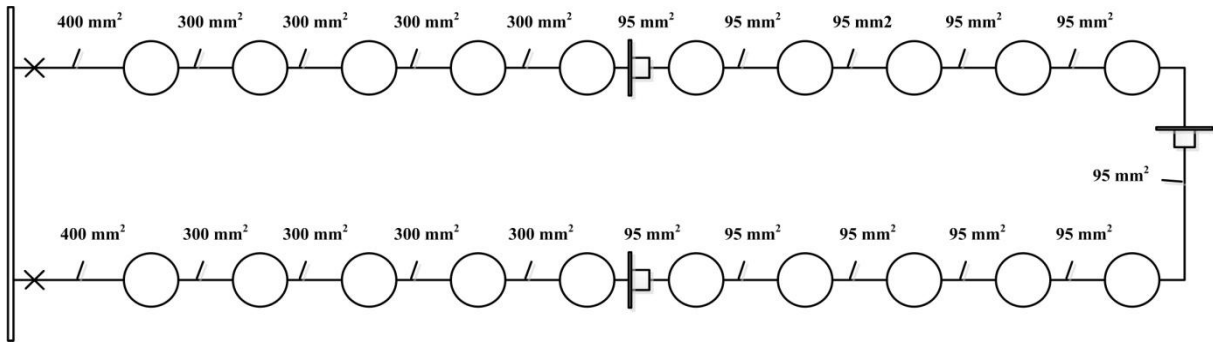


Figure 26. Top.3.  $ENS = 555 \frac{\text{MWh}}{\text{yr}}$

### Alternative layout, Top.4

With load switches placed in the middle the fault can be isolated so that only five turbines will be affected. The circuit breakers and the remote controlled loadswitches can be manouvered in order to isolate the fault. In this layout the cables are dimensioned to bear the load of five extra turbines running on full load. The larger cable dimension also reduces the power losses. The cables are dimensiond for full load conditions which might be a bit exaggeregated since the average power production is about 37 %. On the other hand, the power production is often higher during the winter time due to stronger winds, while the repairtime in case of fault is longer due to problems with access.

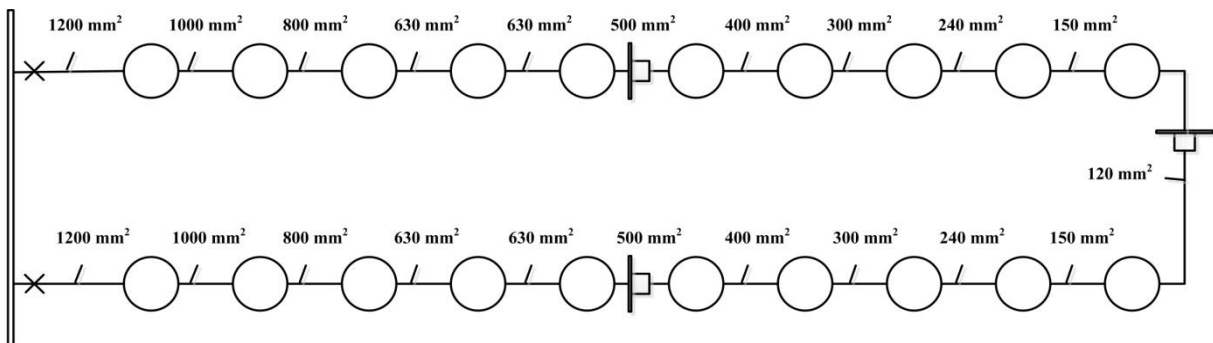
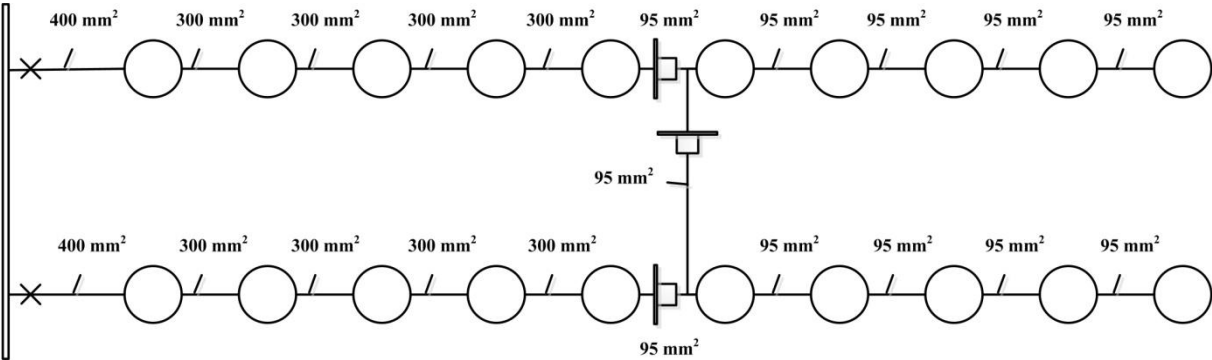


Figure 27. Top.4.  $ENS = 399 \frac{\text{MWh}}{\text{yr}}$

### Alternative layout, Top.5

This topology has the similar function and benefits as Top.3 but the loop is situated in the middle instead of the end of the branches. This alternative provides a large improvement in

case of ENS compared to the original layout but has a bit higher ENS than Top.3. The investment cost is although exactly the same as for Top.3.



**Figure 28. Top.5.**  $ENS = 613 \frac{MWh}{yr}$

**Alternative layout, Top.6**

This topology has the same layout as Top.5 but with higher cable ratings. The cables are dimensioned to manage more load compared to Top.5 but instead the investment cost is higher. This topology provides a huge improvement in ENS compared to the original layout. Top.6 require less modification, compared to the original layout, in contrast to achieve the same value of ENS while implementing the loop in the end of the arrays.

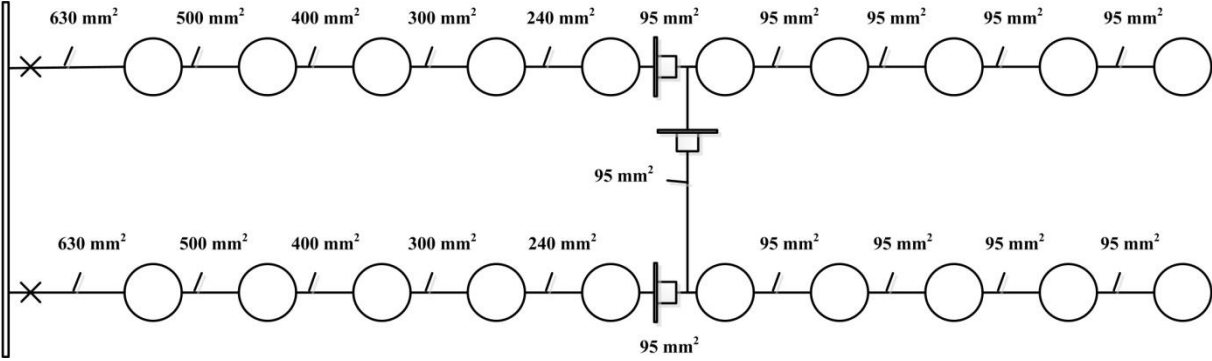


**Figure 29. Top.6.**  $ENS = 448 \frac{MWh}{yr}$

### Alternative layout, Top.7

This topology do not present so much improvements on ENS compared to Top.6 and the investment cost is higher. In comparison to Top.4, which has the same cable ratings in the first halv of the arrays, it present less improvements on ENS. On the other hand, this topology have less investment cost compared to Top.4 and the modifications are less compared to the original layout.

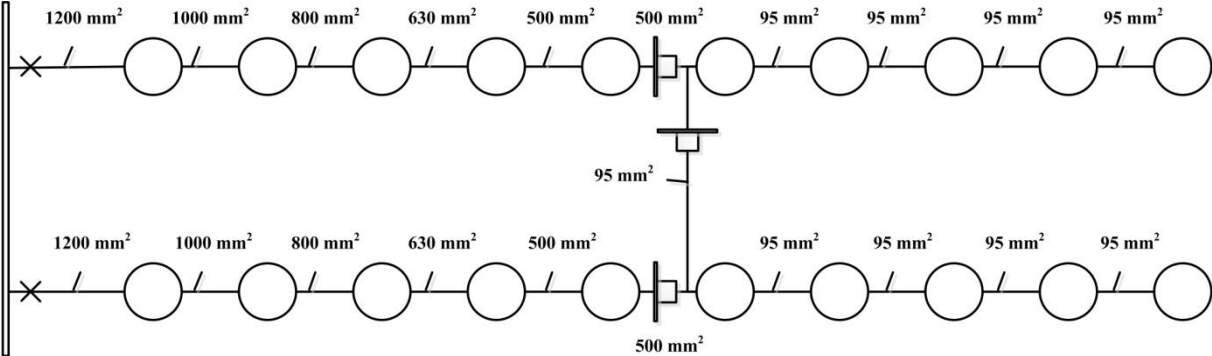


Figure 30. Top.7.  $ENS = 425 \frac{MWh}{yr}$

## CHAPTER 6: Results

*This chapter presents the results obtained from the simulations on different topology alternatives in NEPLAN.*

### 6.1 Description of the results per topology

The previous chapter presents the data used for the models and the different topologies chosen for the analysis. Some drawbacks and benefits are also discussed for each topology chosen. The objective of the study is to perform quantitative reliability analysis on an offshore wind power system including maintenance- and load flow considerations along with evaluations of investment cost. As a base case and used as a benchmark, two arrays of the offshore wind farm Thanet is used. The structure of these arrays will be used as a base case when comparing different topologies against each other. The aim is to present alternative layouts with increased level of reliability at an acceptable cost. The different layouts can be compared in additional

income over the life time of the wind farm, as the energy not supplied (ENS) is used in the study. Seven different topologies are analyzed and compared with respect to the reliability of the different designs. The seven different topologies with diverse level of redundancy are based on various levels of investment costs. The Net Present Value and the Internal Rate of Return are used for investment analysis. The different layouts also consist of different cable ratings which contribute to various levels of power losses for each topology. The Average System Availability Index (ASAI) [%] is presented for each case and it is of interest when evaluating the level of load shedding needed for each topology showing the influence of cable ratings. Figure 31 visualizes the designation of each cable and Table 12 presents the influence of each cable on the overall ENS.

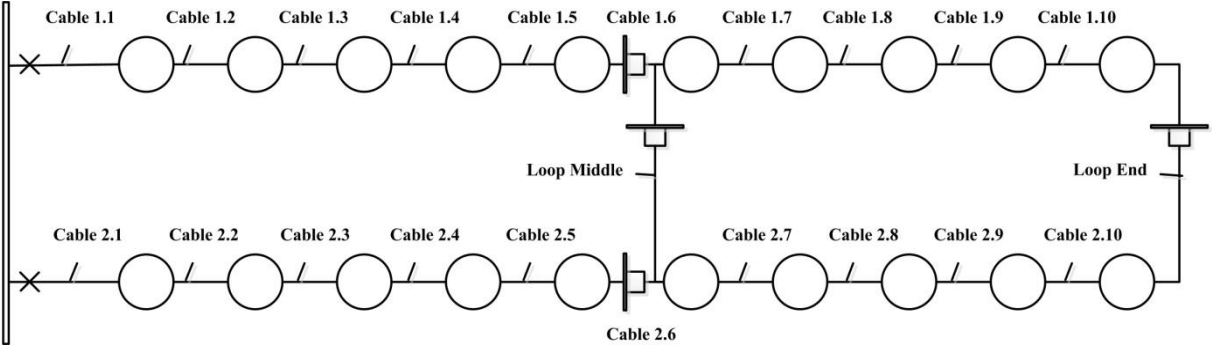


Figure 31. Cable Layout

Different location and function of the cables contributes to different levels of ENS which is visualized in Table 12 below.

Table 12. NEPLAN results and the influence of cables on ENS (case 4)

Name	Type	Top.1				Top.2	Top.3	Top.4	Top.5	Top.6	Top.7
		F [1/yr]	T [h]	Q [min/yr]	ENS [MWh/yr]	ENS	ENS	ENS	ENS	ENS	ENS
**Total**		0,481	170,663	4928,958	2154,533	2143,901	1726,048	1105,927	1999,947	1340,805	1183,595
1.1, 2.1	Cable	0,004	677,151	161,000	79,092	74,886	73,477	32,270	79,171	48,749	35,546
1.2, 2.2	Cable	0,002	679,525	80,427	36,530	34,369	33,670	13,076	36,512	21,313	14,714
1.3, 2.3	Cable	0,002	679,525	80,427	33,552	31,387	30,688	10,093	33,530	18,330	11,732
1.4, 2.4	Cable	0,002	679,525	80,427	30,575	28,404	27,706	7,111	30,546	15,348	8,751
1.5, 2.5	Cable	0,002	679,525	80,427	27,598	25,422	24,724	4,943	27,562	12,366	5,769
1.6, 2.6	Cable	0,002	679,525	80,427	24,621	22,440	17,658	4,905	19,808	8,277	4,911
1.7, 2.7	Cable	0,002	679,525	80,427	21,644	19,459	14,676	4,904	16,830	16,822	16,820
1.8, 2.8	Cable	0,002	679,525	80,427	18,668	16,477	11,695	4,903	13,854	13,843	13,841
1.9, 2.9	Cable	0,002	679,525	80,427	15,691	13,495	8,713	4,902	10,878	10,864	10,862
1.10, 2.10	Cable	0,002	679,525	80,427	12,715	10,514	5,732	4,902	7,902	7,886	7,883
Loop End*	Cable	-	-	-	-	0	0	0	-	-	-
Loop Middle*	Cable	-	-	-	-	-	-	-	0	0	0

\*These cables are modeled as ideal in NEPLAN because they are only used in case of fault and therefore not considered contributing to the average ENS.

The values of ENS for each case and topology are weighted with the probability for each case and a mean value of ENS is presented in bold for each topology.

**Table 13. Based on integration of the product of the probability density function of the wind speed (Rayleigh distribution) (0-25 m/s) and the turbine's power curve (0-3 MW).**

Case	Wind speed [m/s]	Avg. Prod. [MW]	Probability [%]
<b>1</b>	0-3	0	14
<b>2</b>	4-8	0,425	45
<b>3</b>	9-12	1,834	26,5
<b>4</b>	13-25	2,947	14,5

**Table 14.**

Case	Top.1	
	ENS [MWh/yr]	ASAI [%]
<b>1</b>		
<b>2</b>	310,715	99,583
<b>3</b>	1340,826	99,583
<b>4</b>	2154,533	99,583
<b>Avg.</b>	<b>810,168</b>	

Case	Top.2		Top.3		Top.4	
	ENS [MWh/yr]	ASAI [%]	ENS [MWh/yr]	ASAI [%]	ENS [MWh/yr]	ASAI [%]
<b>1</b>						
<b>2</b>	254,744	99,617	148,631	99,760	148,631	99,760
<b>3</b>	1194,423	99,554	890,665	99,620	641,385	99,760
<b>4</b>	2143,901	99,542	1726,048	99,613	1105,927	99,709
<b>Avg.</b>	<b>744,644</b>		<b>555,324</b>		<b>398,555</b>	

Case	Top.5		Top.6		Top.7	
	ENS [MWh/yr]	ASAI [%]	ENS [MWh/yr]	ASAI [%]	ENS [MWh/yr]	ASAI [%]
<b>1</b>						
<b>2</b>	187,520	99,748	157,213	99,748	157,213	99,748
<b>3</b>	890,679	99,705	684,405	99,725	684,405	99,725
<b>4</b>	1999,947	99,613	1340,805	99,613	1183,595	99,690
<b>Avg.</b>	<b>612,850</b>		<b>448,161</b>		<b>425,175</b>	

Table 15 shows the possible additional energy production and income for each topology. The possible total extra income over the lifetime of 20 years is also calculated by multiplying the additional income per year with 20 and then subtracting the additional investment for each topology. These figures do not consider any fluctuations in electricity price, discount rate and inflation rate.

**Table 15. The additional annual energy that can be supplied for different topologies.**

Wind farm topology	Average ENS [MWh/yr]	Add. Energy that can be supplied [MWh/yr]	Add. Income per year [k€]	Add. Investment [k€]	Total Extra income (20 years) [k€]
<b>Top.1</b>	810,168				
<b>Top.2</b>	744,644	65,524	11,794	289,000	-53,113
<b>Top.3</b>	555,324	254,844	45,872	309,000	608,438
<b>Top.4</b>	398,555	411,613	74,090	1571,087	-89,280
<b>Top.5</b>	612,850	197,319	35,517	309,000	401,347
<b>Top.6</b>	448,161	362,007	65,161	474,848	828,379
<b>Top.7</b>	425,175	384,994	69,299	1158,685	227,292

The Table 16 presents the Net Present Value and the Internal Rate of Return for each topology. According to the results of NPV and IRR there are three alternative topologies which provide positive values and therefore are worth considering when constructing an offshore wind farm with similar conditions. Top.7 also present a positive value of IRR but since  $IRR < WACC$ , (i.e. discount rate,  $r$ ) it should be discarded.

**Table 16. This shows if the additional investments will be beneficial related to additional cash flow.**

Duration t, years	Discount rate, r	Layout	Add. Investment [k€]	NPV [k€]	IRR [%]
t=20 years for all topologies	r = 7 % for all topologies	<b>Top.2</b>	289,000	-153,32	-2
		<b>Top.3</b>	309,000	165,390	14
		<b>Top.4</b>	1571,087	-734,741	-1
		<b>Top.5</b>	309,000	62,870	10

		<b>Top.6</b>	474,848	201,376	12
		<b>Top.7</b>	1158,685	-396,759	2

Figure 32 shows how much the average energy not supplied varies between the different topologies. It also provides an indication of how reliable each topology is. Figure 33 presents the additional investment each topology requires in order to achieve the extra redundancy compared to the original layout. Figure 34 presents the results from the investment analysis and visualizes the net present value for each topology alternative. One can clearly see that Top.3, 5 and 6 provides positive NPV.

Figure 32

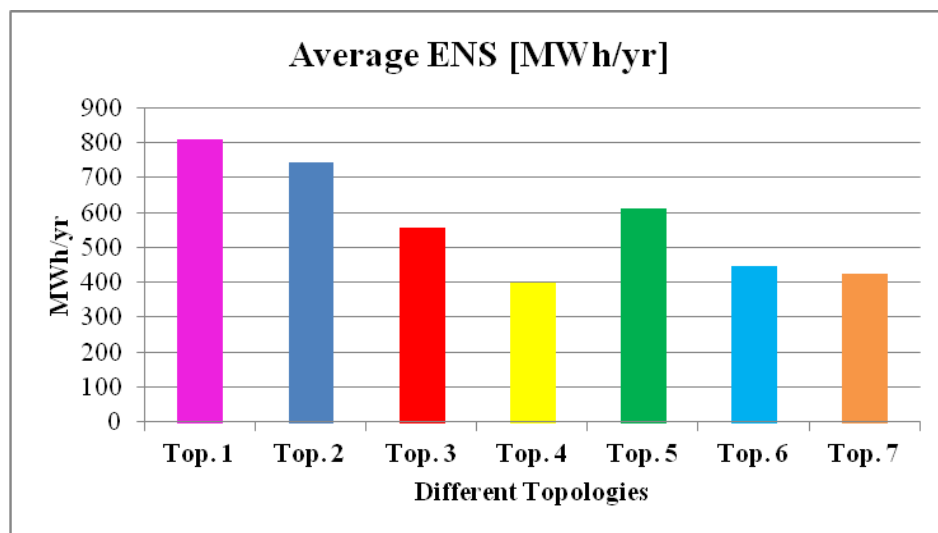


Figure 33

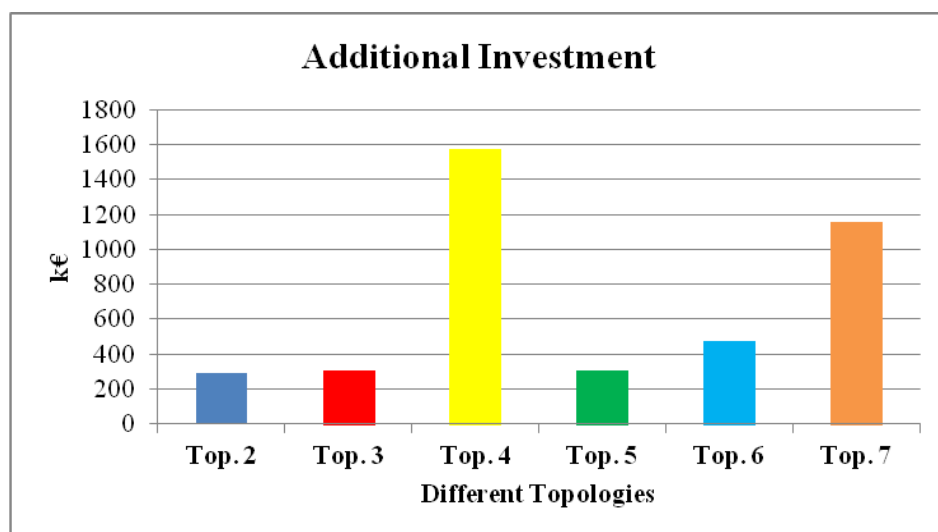
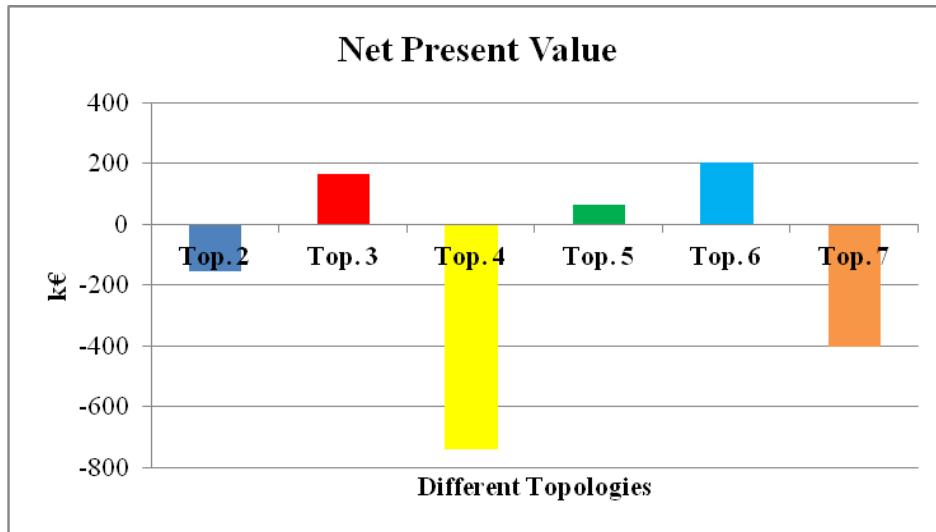


Figure 34



## 6.2 Results discussion

The probability of production is quite rough divided in four cases which might have an influence on the results. In order to mimic a more realistic scenario with dynamic load, more cases could have been utilized. The four cases are though a good approximation suitable for the study. Related to the probability of production, it can be observed in Table 13 that the turbines actually produce zero power with the probability of 14%. This is almost as high probability as for the rated power production.

Top.4 and 7 are the topologies with the highest cable ratings, and entails in this case the lowest contribution to ENS. These two topologies also have the highest investment cost and provides the lowest value of NPV, and therefore not considered as an investment alternative. The topologies with as high cable ratings as 1200 mm<sup>2</sup> might have even higher investment cost in the reality. This could be caused by the non standard ratings of the cables along with other difficulties with large cables such as transportation and connection.

Top.6 has higher cable ratings compared to the original layout but the cables are considered practically feasible and it provides a huge improvement in ENS. The investment cost is not so high, it presents the highest NPV and is therefore considered as the best alternative for investment when constructing a new offshore wind farm. Observing Table 14 it can be seen that the availability is the same for Top.6 and 7 in case 3 which is the most probable of the four cases.

As mentioned earlier in the thesis, the offshore wind industry is a recent industry with a low maturity which leads to difficulty in estimating failure rates for subsea cables. The site of the

offshore wind farm is also of importance related to this because the largest contribution of external influence on subsea cables is caused by anchors.

Failures are more likely to occur in the beginning- and in the end of the components life time and the failures occurring in the early beginning after commissioning the offshore wind farm have a high impact on the NPV.

## CHAPTER 7: Conclusions

---

*This chapter concludes the thesis, summarizes the results, present some ideas and discusses future work.*

---

### 7.1 Conclusions and discussion

The main objectives of this study were to evaluate different layouts for the internal grid of an offshore wind farm with respect to reliability, investments and maintenance- and considering cable constraints. For this analysis a model was constructed as a benchmark and the software NEPLAN was utilized as a working tool. The aim of the presented results was to highlight weak spots of the collector system and how different layouts with various cable ratings contribute to a variety of ENS. Further aim of the presented results was to convert the possible additional energy production into Euros and perform a cost benefit analysis. This is shown by calculating the NPV and for the input data used in the report, three of the six investigated topologies, i.e. Top.3, Top.5 and Top.6, had a positive NPV.

As stated previously in the report it is difficult to collect trustworthy reliability data and the figures can vary extensively between manufacturers and construction sites offshore. Installation cost and prices on different cable ratings and switchgear also vary between manufacturers and over time with variations in metal prices. Another aspect to consider when evaluating the results is fluctuations in income from produced electricity, where different subsidies and the price per kilowatt hour vary over time. It is important to beware of all these aspects when using the model for assessing the system performance and evaluating investment alternatives.

### 7.2 Future work

For future studies it would be interesting to refine the model even more and include some realistic and practical details. The model in this report does for example not consider practical limitations and difficulties of using large cable dimensions. For very large cable dimensions it could be problems with weight during transportation and installations of the cables. Another aspect concerning large cable dimensions is the connection point, and the cables might have

to be reduced in dimension before connection. When using a cable loop in the middle like Top.5, 6 and 7 it might need further investigation whether the connection point inside the turbine is suitable for three connection points and additional switchgears.

Another aspect to investigate in future studies could be whether an increase in cable ratings also could have more benefits over time with less risk of failure due to thicker layer of insulation, less stress elicited by power flow and less power losses.

As a consequence of several parameters included in the model with uncertainties; a sensitivity analysis should be performed. A sensitivity analysis can provide an indication of how sensitive the results from the analysis are, when one or more input parameters changes in values.

The constructed model for this study only consider to arrays with ten turbines and it would be of interest to expand the model to include a complete wind farm with hundred turbines like Thanet. In this case more topologies could be investigated and more than two arrays could be connected together with loops in between. For such alternative it would be interesting to include more statistical data in the model of for example how likely it is for failure to occur in to arrays at the same time. The topology of e.g. Thanet may be more complex due to the bathymetry and it could be interesting to investigate how such complexity may influence the benefit of redundancy; however, this is a case per case situations.

## References

- [1] Billinton, R., Allan, R. N., *Reliability evaluation of power system*, Plenum Press, 2nd edition, 1996
- [2] Billinton, R., Wenyan, L. *Reliability Assessment of Electric Power Systems Using Monte Carlo Methods*, Plenum Press, 1994.
- [3] [www.neplan.ch](http://www.neplan.ch)
- [4] Presentation of Neplan reliability, Math Bollen, STRI AB, Ludvika, Sweden, 2007.
- [5] Neplan User's guide, Technical report.
- [6] Frankén, B., STRI AB, *Reliability study – Analyses of electrical system within offshore wind parks*, Technical report, Elforsk, 2007
- [7] European Wind Energy Association, *Oceans of Opportunity, Harnessing Europe's largest domestic energy resource*, 2009
- [8] Wizelius, T., *Vindkraft i teori och praktik*, Studentlitteratur, Sweden 2007
- [9] Mousavi Gargari, S. *Reliability Assessment of Complex Power Systems and the Use of NEPLAN Tool*, Master Thesis, Royal Institute of Technology, RCAM research team, 2006.
- [10] Eriksson E. *Wind farm layout, a reliability and investment analysis*, Master Thesis, Uppsala University, 2008.
- [11] Sannino A, Breder H, Kolby Nielsen E, *Reliability of Collection Grids for Large Offshore Wind Parks*, 2006
- [12] Frankén, B., STRI AB, *Reliability study – Analyses of electrical system within offshore wind parks*, Elforsk report, 2007
- [13] [www.vestas.com](http://www.vestas.com)
- [14] Tidwell J., Gaudiosi G., *Offshore Wind Power*, Multi-Science Publishing Co. Ltd, 2009.
- [15] Besnard F., *On Optimal Maintenance Management for Wind Power Systems*, Licentiate Thesis, 2009.
- [16] Blaabjerg F., Chen Z., Teodorescu R., Iov F., *Power Electronics in Wind Turbine Systems*, Aalborg University, Institute of Energy Technology, 2006
- [17] Holmstrøm, O. *Reliability of state-of-the-art wind farms*. Project UpWind, Technical report, 2007.
- [18] Quinonez-Varela, G., Ault, G.W., Anaya-Lara, O., & McDonald, J.R. *Electrical collector system options for large offshore wind farms*, 2007.
- [19] DOE, EERE Web site. <http://www.eere.energy.gov>
- [20] [www.vattenfall.se](http://www.vattenfall.se)

- [21] [www.siemens.com](http://www.siemens.com)
- [22] Download press photo: [www.siemens.com/Transmission/pictures/EPT200809064](http://www.siemens.com/Transmission/pictures/EPT200809064), Rights for using the picture has been received by Siemens AB Corporate Communications.
- [23] [powerplants.vattenfall.com/powerplant/thanet](http://powerplants.vattenfall.com/powerplant/thanet)
- [24] Offshore Wind in Europe, *Energy & Natural resources*, (pp.10), KPMG Market Report, 2010
- [25] Manwell J.F., McGowan J.G., Rogers A.L., *Wind Energy Explained Theory, Design and Application*, John Wiley & Sons Ltd, 2009.
- [26] Discussion with Francois Besnard, Ph.D. student at Chalmers university of Technology and O&M analyst at Vattenfall Wind.
- [27] [www.alpha-ventus.de](http://www.alpha-ventus.de)
- [28] Mason G., *Development, Design and Construction of Offshore Windfarms*, Presentation, 2009.
- [29] Eugene F. Brigham, Michael C. Ehrhardt, *Financial Management Theory and Practice*, 2010.